Uranium metallogeny in the North Flinders Ranges region of South Australia

Pierre-Alain Wülser

Department of Geology and Geophysics
Adelaide University

This thesis is submitted in the fulfilment of the requirements for the degree of Doctor of Philosophy in the Faculty of Science, Adelaide University

June 2009

THE UNIVERSITY OF ADELAIDE
AUSTRALIA

PART TWO

Metallogeny of uranium and thorium in the Mount Painter Domain

(North Flinders Ranges, South Australia)

4 Mineralogy, petrography and geochemistry

4.1 The Yerila granite complex, Mount Babbage Inlier

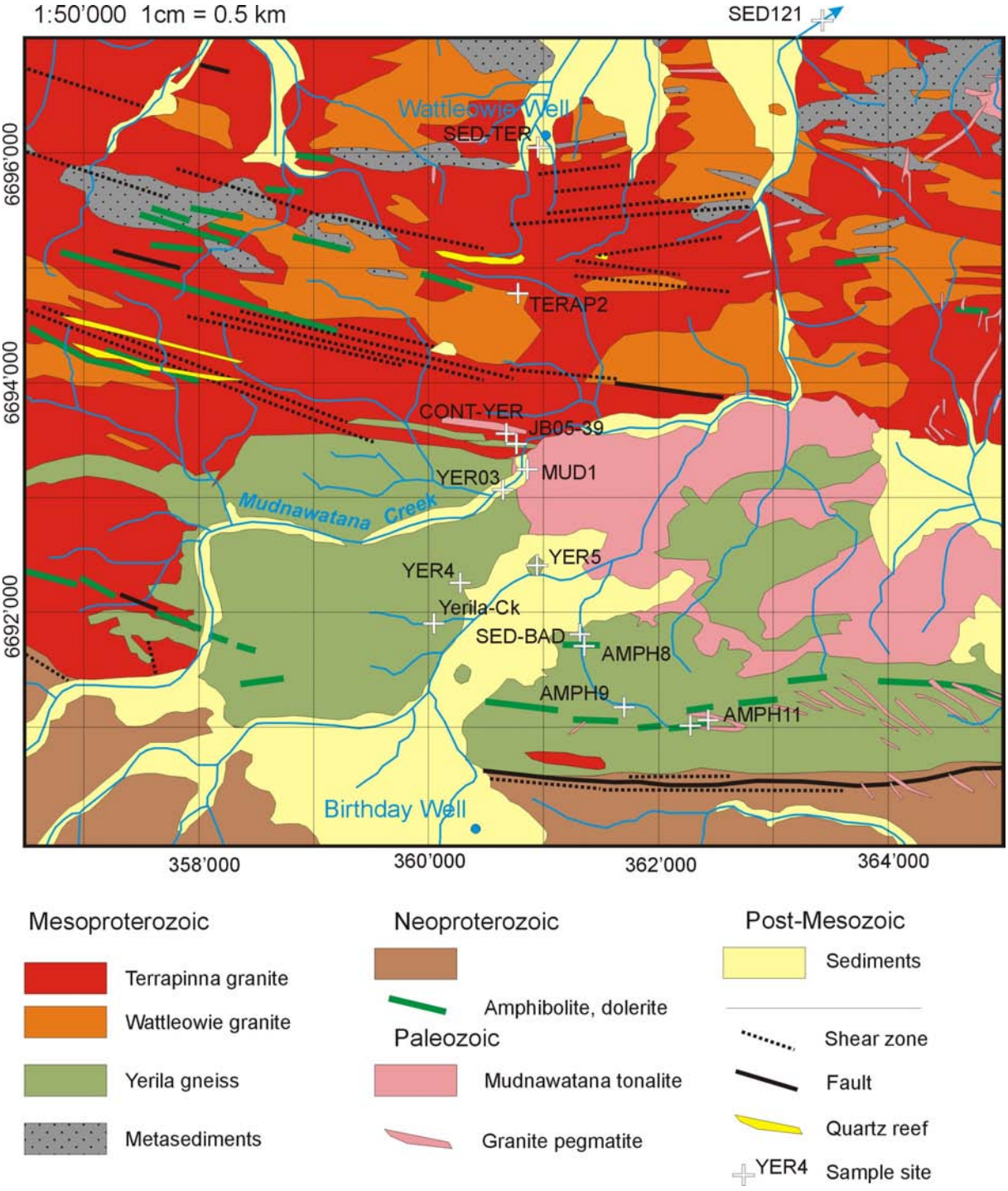

Fig. 10: Geologic map of the studied area in the Mount Babbage Inlier (MBI)

All rock samples are located between Birthday and Wattleowie wells. HM concentrates from sediments are SED-BAD, SED121, AMPH9 and Yerila-Ck. YER03 as been selected as a very characteristic rock sample for the main Yerila granite.

The Yerila granite sensu stricto forms a discontinuous elongate body of porphyritic K-feldspar, biotite granite gneiss measuring approximately 14 km on 3-4 km (see location 4 on Fig. 7). Its shape was precisely mapped on the 1961 and 1969 maps. The rock was named after the Mount Yerila (originally called "Ehrenbreitstein" until 1918), 12 km to the North in the plain. The radiometric maps also nicely correlate the outcrops, displaying high intensity gamma signals (Th & U). The studied area is located on its Western section, north of Birthday Well. The Southern limit of the body forms a linear eroded surface with the Adelaidean Sturtian tillites; these tillites are conglomeratic and pebbles to boulders are essentially derived from the local MPD granites (Terrapinna granite, mostly). The Yerila granite is in direct contact with the Terrapinna granite on most of its Western and northern limits. The central body is intruded by the Paleozoic (Presumably Ordovician) Mudnawatana tonalite or granite. Numerous granite pegmatites also crosscut the gneiss with a general direction trend NW-SE. Both Terrapinna and Yerila are crosscut by amphibolite dikes, which can be followed on tens of kilometres. These dikes have been interpreted as Neoproterozoic. They are themselves cut by the granite pegmatites. The Yerila granite is not uniform and is interlayered by lenses and sheets of allanite-rich calcsilicates and biotite schists.

4.1.1 The Yerila granite

YER-03:

The Yerila granite is generally composed of large tabular K-feldspar phenocrysts and abundant biotite. A large sample of this main type (25 kg) was collected in 2003: YER-03. The rock is porphyritic, gneissic with orientated large laths of K-feldspars (up to 4 cm), large allanite patches (2-8 mm) and light brown radioactive patches (1-2 mm) forming radial cracks in the surrounding matrix. The abundance of biotite gives a general dark aspect to the outcrops. K-feldspars are microfractured transversally and the cracks filled by quartz-feldspar veinlets with minor biotite and fluorite as visible on the polished rock on Fig. 11. Phenocrysts are orthoclase with simple twinning; they often show the grid twinning of microcline that may have been induced by stress. Less commonly, phenocrysts of oligoclase occur, incipiently sericitised and with fine biotite inclusions, giving a macroscopic grey colour. The matrix is formed of microgranular quartz and K-feldspar and biotite, titanite and an alkaline amphibole: hastingsite. Fluorite occurs disseminated as small dark purple crystals throughout the rock. Accessories by order of abundance are titanite, allanite (rimmed by epidote-zoisite), fluorite, apatite, black zircon of alkaline morphology "D" and minor "K" (see also Fig. 12 and sample Yerila-Ck) and very little ilmenite. Additional heavy mineral concentrates were prepared and further accessories identified and separated: uranothorites, uraninite, molybdenite, sphalerite, powellite, scheelite, bastnäsite-synchysite, chevkinite, pyrite and arsenopyrite. Magnetite is totally absent in the heavy mineral concentrate and rare ilmenite rimmed by titanite occurs.

Fluorite seems to have crystallized early in the sequence, so do some hastingsite (poikilitic texture) intergrown with biotite. However, hastingsite dominantly crystallized late in the sequence with most of the biotite (i.e. post-stress). Most accessories are included in the late-stage biotite (numerous radioactive inclusions forming halos) or at mineral boundaries. Purified quartz fractions (up to 92 Wt-% SiO_2) still host 180 ppm Zr, documenting the general dispersion of zircon as inclusion throughout the entire rock assemblage.

YER5:

The rock is granitic in composition, with a stressed gneissic fabric. Phenocrysts of quartz, albite and orthoclase are modified and lie in a silicified matrix of quartz, albite with minor chloritized biotite. The typical laths of microcline present in YER-03 are completely absent. Late-stage muscovite occurs in fractures. Accessory minerals are zircon, ilmenite, apatite, pyrite, totally altered allanite and molybdenite, thorite, bastnäsite and titanite. Very minor calcite and fluorite occur as late stage minerals; titanite is granular and replaces early ilmenite. Allanite is porphyroblastic and crystallised late in the sequence. Magnetite is totally absent in the heavy mineral concentrate. Figure 11 provides a good estimates of the composition (K-feldspar phenocrysts are white); the grey-green granular matrix is composed of albite and quartz essentially. The presence of late-stage allanite, fluorite, titanite, as well as the abundance of albite indicate that the rock was subject to an alkali remobilisation (sodium metasomatism) different from Yer-03. Most of the original textures were not preserved. The composition of the rock is Na_2O-rich (7.18 Wt-%) and silica-rich (75.4 %), corresponding to a monzogranite-granodiorite; the HSFE patterns and mineralogy are identical to YER-03 for: 160 ppm U, 480 ppm Th, 110 ppm Nb, 250 ppm Y, 470 ppm Zr, but much lower REE (completely altered allanite). The presence of late-stage calcite-fluorite veinlets, the presence of preserved ilmenite, pyrite and molybdenite also indicates the metasomatism here was not oxidising. By comparing YER03 and YER5, the main difference is the biotite content and the albite-quartz in the other.

JB05-39:

The Yerila granite JB05-39 is localised close to the northern limit of the massif, adjacent to the Terrapinna granite. The gneiss extremely rich in biotite (40%) and the K-feldspar laths typical of Yerila are present. Porphyritic K-feldspars are coarse and fractured; and quartz is stressed, veined by quartz-biotite-K-feldspar veinlets. The matrix is composed of granular quartz, K-feldspar, plagioclase and strongly foliated dark biotite. Accessory minerals are titanite (radioactive & non-radioactive), apatite, zircon, fluorite and completely decomposed allanite surrounded by

radial fractures (up to 5 mm in diameter). The biotite hosts numerous radioactive mineral inclusions. Black oxides (ilmenite or magnetite) are totally absent. The rock was subject to a dynamic metamorphism with limited recrystallisation; this observation is probably linked to the vicinity of the Paleozoic intrusive close-by (150 m away). Like in YER-03, most biotite crystallised late in the sequence and accounts for almost all the iron from the whole-rock composition. Microscopic measurements indicate the biotite is close to the annite end-member. The chemical composition of the rock has high Zr (1000 ppm), Y (250 ppm), Nb (86 ppm), Th (375 ppm), U (40 ppm) and REE: 1190 ppm Ce, 650 ppm La and 500 ppm Nd. These concentrations are due in part to allanite but particularly to concentrations of apatite, zircon and thorite in the biotite layers. The late crystallisation of biotite can be explained by the high-fluorine content of the rock.

CONT-YER

The gneiss is a porphyritic, with microcline phenocrysts in a coarse-grained matrix of quartz, microcline and albite. Dark biotite form subparallel flakes. The major components show strain-extinction. The observed accessory minerals are: subhedral apatite, irregular titanite, zircon (both euhedral and rounded), ilmenite. The biotite contains numerous zircon inclusions. CONT-YER is located close to JB05-39 and in the direct proximity of the Mudnawatana intrusion. A W-E shear zone occurs 50 m to the north. Although the rock present morphological similarities with the nearby Yerila granite, the rock is devoid of allanite. Only Zr has an elevated concentration (935 ppm Zr). Other elements are still high but without extreme concentrations: 50 ppm Nb, 107 ppm Y, 11 ppm U, 34 ppm Th, 237 ppm Ce. The rock marks a transition between the Yerila granite and the adjacent Terrapinna granite/Wattleowie granite. The presence of rounded zircons together with the lack of Zr-Th-U-REE typical association from the Yerila granite indicates the rock has sedimentary in origin.

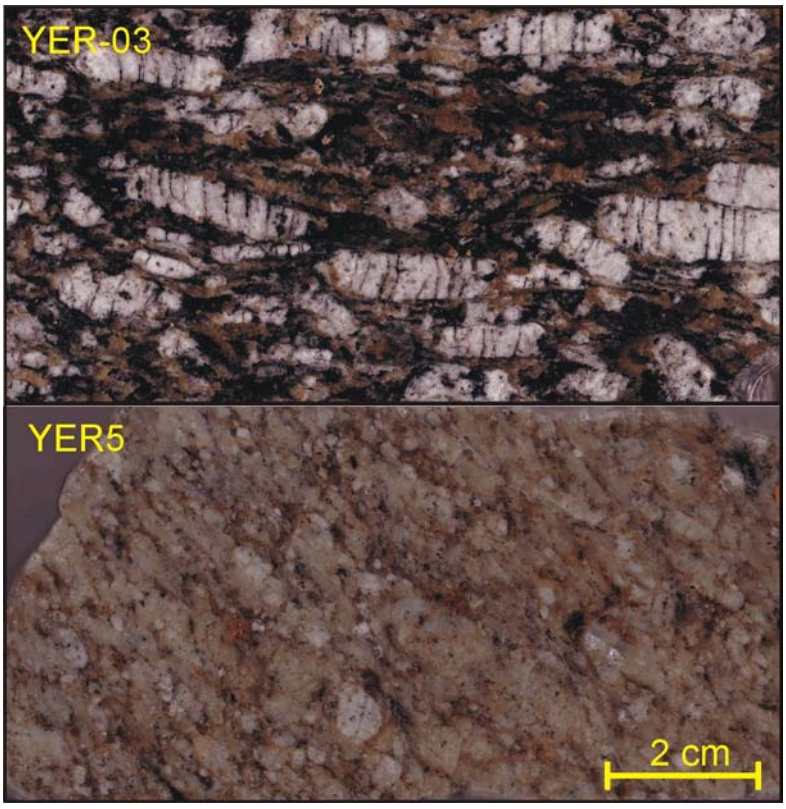

Fig. 11: Polished rock samples of Yerila granite YER-03 and YER5

The two rocks show similar trace element patterns but differ significantly in major minerals. YER5 is dominated by albite and quartz with altered allanite and biotite remnants. YER-03 is microcline, biotite and quartz dominant with minor oligoclase. Biotite is rare in YER5 and was partly chloritised

4.1.2 The Paleozoic intrusives

MUD1

The Mudnawatana "tonalite" intrudes the Yerila granite and a sample was taken from a fresh outcrop close to the western extremity of the main body. The granite is a white medium-grained fresh looking, undeformed rock. Euhedral, zoned, poorly-twinned crystals of oligoclase are embedded in poikilitic, stressed quartz, with very minor

interstitial microcline. Fresh brown biotite flakes are randomly scattered through the rock and contain small pleochroic haloes due to zircon and apatite. Minor muscovite (phengite) replaces cores of oligoclase crystals. Some of the plagioclase is anthiperthitic. Accessory mineral are apatite and zircon. The rock composition should be described as trondhjemite but not tonalite.

4.1.3 Heavy minerals from stream sediments

Yerila-Ck

The sample Yerila-CK was collected in 2003 during the first investigation and is composed of 4.8 kg of alluvium collected in a narrow medium-slope gully draining exclusively the main Western Yerila body. This sample hence provides a representative view of the mineralogical diversity of the Yerila granite, including its minor lithologies. The heavy minerals recovered by panning were observed and sorted using SEM and binocular microscopes. The following petrologic types have been observed in the coarse fragments: diverse gneisses, quartz, calcrete pebbles.

The observed mineralogy is: quartz, K-feldspar, biotite, muscovite, magnetite, ilmenite, zircon, fluorite, apatite, hornblende, xenotime, monazite, dravite and abundant scheelite. Rarer minerals are: titanite, allanite, rutile, elbaite, chrysoberyl, bismuthinite, spessartine, molybdenite, epidote, euxenite-(Y), fergusonite-(Y) and columbite. The zircons are exceptionally large (up to 4-5 mm) and black, brown or orange. The zircon typology was studied and is reported in Fig. 12. It shows the predominance of D type, with lesser amounts of P3-5 and K types. A typical K zircon from Yerila-Ck is commented on Fig. 13. Occurrence of this type of zircon is restricted to alkaline series granites and granitoids (Pupin, 1980). The absence of well-rounded colourless zircons or S types witnesses the absence of other rock unit or Mesozoic sedimentary cover in the watershed. The magnetite and the scheelite are interpreted to be issued from calc-silicate layers.

SED-BAD

The sample SED-BAD was taken from a naturally concentrated heavy mineral pocket in the bed-rock of a small creek. The size of the watershed is 1.5 km². The coarse fraction was examined for petrographic types and the following rock types were observed: 52% Biotite gneiss (Yerila), 35% granite pegmatite, 7% of amphibolite, 6% of calcrete pebbles. 1.4 kg of <5 mm sand was used for the heavy mineral preparation. Due to large amount of HM recovered, a detailed quantitative analysis of the mineralogy was undertaken. The mineral diversity found in the HM's is unusually rich and rare mineral species are common, especially those containing cerium (Table 3).

Magnetite (7.94 g)	Rutile, ilmenorutile (0.02 g)	Coronadite (1 g)
Ilmenite, minor hematite (4.66 g)	Columbo-tantalite (42 grains) (0.01 g)	"Ce-rich hollandite" (3 g)
Monazite.70%, xenotime 30% (2.59 g)	Euxenite, fergusonite, microlite (14 g)	Cerianite (3 g)
Garnet (Alm-Spes.) (0.72 g)	Cerite-(Ce) (10 g)	Bismuthite (3 g)
Zircon (0.32 g)	Allanite-(Ce) (8 g)	Cassiterite (2 g)
Apatite, fluorite, elbaite (0.11 g)	Barite (5 g)	Torneböhmite-(Ce) (1 g)
Scheelite (0.04 g) (~ 30 ppm W)	Hollandite (4 g)	
Törnebohmite-(Ce): $Ce_2Al(SiO_4)_2(OH)$ (Ce>>La)	*Fluocerite-(Ce): $(Ce_{0.45}La_{0.42}Nd_{0.09}Pr_{0.03})F_3$*	*Cerium-rich hollandite: $(Ba,Ce)(Mn^{4+}\ Mn^{2+})_8O_{16}$*
Cerite-(Ce): $(Ce,Ca)_9(Mg,Fe)Si_7(O,OH)_{28}$	*Cerianite-(Ce): $(Ce^{4+},Th)O_2$*	*Coronadite, hollandite: $(Pb,Sr,Ba)(Mn^{4+}Mn^{3+})_8O_{16}$*

Table 3: Mineralogy of the SED-BAD HM concentrates

The minerals were picked and then examined by SEM for unusual element identification. When mineral phases are large, the fractions were weighted, otherwise grains counted. The mineralogy shows some extremely rare mineral species, especially minerals containing cerium. The chemical formulae of the cerium-rich minerals are reported at the bottom of the table.

The zircon typology is reported in Fig. 12. Determined types correspond to alkaline zircons exclusively.

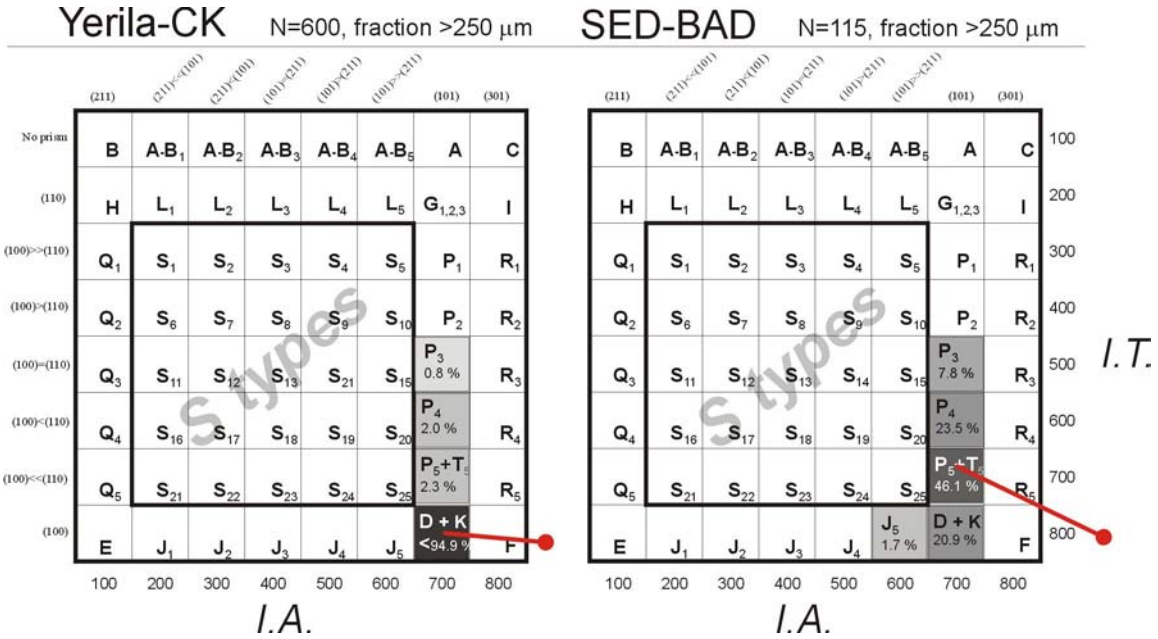

Fig. 12: Zircon typology grids for Yerila-Ck and SED-BAD

The zircon typology indicates both samples are of alkaline granite series. They also display high temperatures index I.T., the average T on a single zircon population, is 792 for Yerila-CK and 684 for SED-BAD.

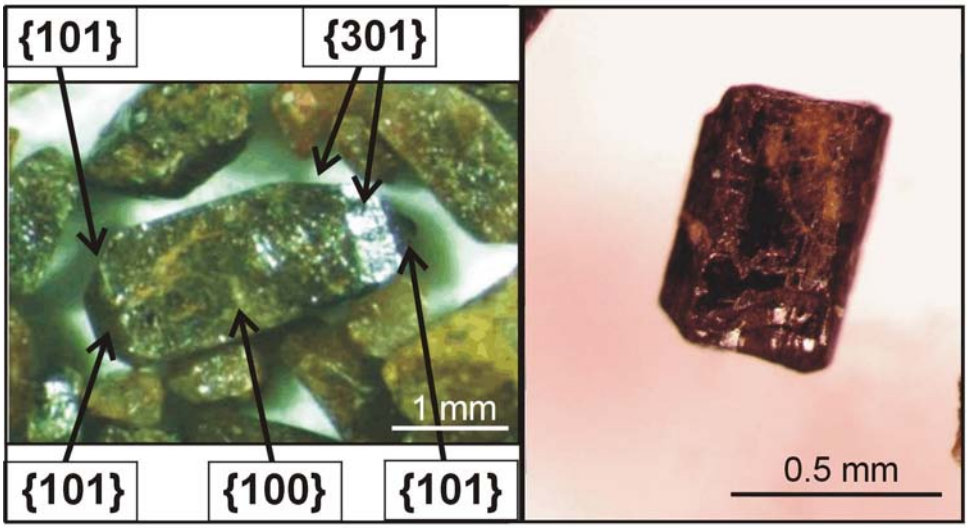

Fig. 13: "K"-type zircon from Yerila-Ck and quadratic columbite prism from SED-BAD

(Left): the two pyramids occurring are [301] and [101]. This type of zircon is only restricted to the granites from the alkaline series and with hot dry magmatic genesis (Pupin 1980); it is met in particular in hypersolvus alkaline granites with typical string perthites. (Right): A fresh unworn black columbite crystal from SED-BAD combining two prisms [100] and [110]

AMPH9

The sample AMPH9 was collected upstream the sample SED-BAD in a small gully draining around 0.13 km² of watershed. The sediment was collected directly against the bedrock in a flat, just a few meters downstream from an amphibolite dike. The heavy mineral assemblage by order of importance is: ilmenite, monazite, spessartine-almandine, xenotime, zircon and scheelite. Hornblende is also abundant in the concentrates and can be considered as a heavy mineral (d~3.1 g/cm³). Less common minerals are tourmaline, cerite, columbite, fergusonite, hollandite,

euxenite, and magnetite. The monazite and the xenotime are very abundant and represent more than 30% of the total HM's. They frequently reach a few millimetres (up to 4-5 mm). Xenotime and monazite form twinned crystals, and both have been observed attached to a gneissic (quartz-biotite) rock matrix, which indicates they do not originate from the local pegmatites. Some crystals are exceptionally fresh and yellow transparent. Garnets have been observed in the nearby pegmatites dikes. Scheelite is present as coarse grains with very angular shape. Zircons are brown to orange in colour and their typology is centred on the "P5" subgroup of Pupin, typical for alkaline series granites (Fig. 12).

SED121

The sample SED121 is located out of the map in Figure 10. It was collected in the Mudnawatana Creek, the main watershed for Yerila and Terrapinna, also draining some metasomatised dolomitic Adelaidean sediments from the Mount Fitton area. The heavy mineral concentrate was studied to provide a comparison to the mineral assemblages collected in other samples upstream.

The following mineralogy was recorded (from the commonest to the rarest): garnet, ilmenite, tremolite, hornblende, hematite, magnetite, monazite, allanite, apatite, xenotime, zircon, tourmaline, columbite, scheelite, fluorite, blue anatase, cerite-(Ce) and hollandite. Zircons are of mixed origins: black "D" zircons from Yerila, elongated colourless zircons with black oxide inclusions and melted-like surfaces. These zircons probably come from the Wattleowie granite (S-type granite) and certainly are older than 1600 Ma. Xenotime appears both with prisms like zircons or without as dipyramids (flattened octahedrons). The presence of rare minerals like cerite, hollandite, scheelite and columbite, around 6 km downstream the first outcrops of Yerila granite is interesting and implies that these minerals are relatively widely distributed in Yerila and not just on the studied locations upstream.

4.1.4 Mafic dikes

AMPH10/11/09:

The Mount Babbage Inlier is intruded by numerous ESE trending mafic dikes. These range from amphibolites with locally coarser gabbroic textures. They are themselves crosscut by the Paleozoic pegmatites and the age has been interpreted to be Neoproterozoic, similar to the Wooltana Volcanics to the SE of the MPD (Preiss *et al.* 1993).

The main amphibolite dike was investigated at AMPH10 and AMPH11 for both geochronology and geochemistry. A few kilograms were crushed and heavy minerals separated.

Main minerals observed are hornblende and plagioclase. Quartz is absent. The hornblende forms stubby laths interspersed with fresh andesine-labradorite plagioclase crystals. The main HM is ilmenite with a total absence of magnetite in both samples. Apatite and rutile are rare. Even rarer are polycrystalline "cauliflower zircon" and zircons aggregates. This correlates with low Zr values (100 ppm) and very low Y (26-30 ppm) and REE (22 ppm Ce). They also display high Ni (100-120 ppm) and Cr (260-300 ppm) contents. Most trace and major elements diagrams indicate a tholeiitic basalt signature. Analyses are reported in Appendix III.

4.1.5 Mineral and rock chemistry

YER-03:

Microprobe analyses of all mineral species from YER-03 are shown in the Appendix II. Data are available for allanite, amphibole, titanite, apatite, feldspars, biotite, zircon, REE-fluorocarbonates, euxenite, thorite, uraninite and chevkinite. Only representative figures and mineral formulae are given in this section.

The K-feldspar is microcline; studies by X-ray diffraction by Johnson (1980) indicate a triclinic maximum microcline; its average composition is $K_{0.955}Na_{0.045}AlSi_3O_8$ with ~1150 ppm Ba (XRF data). The plagioclase average composition is An29.2, $Na_{0.701}Ca_{0.292}K_{0.006}Al_{1.22}Si_{2.78}O_8$, in the oligoclase field. The analysed phenocrysts (n=18) range from An26 to An32. The phenocrysts host numerous inclusions of all types. The phenocrysts bear transversal cracks generally containing crystals of biotite and fluorite. Clots of biotite (up to 1 mm) occur in the large microcline laths.

Biotite composition is Fe-rich, close to the annite end-member. The compositions are reported on Figure 14e, in an Al_{TOT} versus Mg (apfu) diagram showing the field of occurrences of biotite in granitoids (Nachit *et al.*, 1985). The average composition gives the following formula:

$$[K]_{0.97}[Fe^{2+}_{2.05}Mg_{0.51}Ti_{0.12}Mn_{0.02}Al^{3+}_{0.33}]<Al_{1.07}Si_{2.93}>O_{10}[(OH_{1.82}F_{0.18}].$$

The biotite compositions plot in the field of the peralkaline or alkaline granite suites (A-type), with a high Fe composition: 28-30 Wt-% FeO. Most of the available iron in the rock resides in biotite.

The second ferromagnesian mineral by volume is a calcic alkaline amphibole. The amphibole is a potassic-hastingsite, with a solid solution toward a ferro-tchermakite or ferro-ferri-tchermakite (according to the current amphibole IMA nomenclature (Hawthorne and Oberti, 2006)). Despite the high fluorine content in the rock, the amphibole is

hydroxyl- dominant and chlorine remains a minor element. The composition was investigated by EMPA and additional bulk XRF and spectrophotometry Fe^{2+} determinations were made on pure mineral concentrates ($d>3.32$ g/cm^3, 0.27-0.34 Ampere on the Frantz separator). The compositions reported on the diagrams in Fig. 14a to Fig. 14d lie in the incertitude of each other, meaning the mineral composition is homogenous in the rock. The composition gives the following formula:

$$^{A}[K_{0.44}Na_{0.21}]_{\Sigma=0.65}{}^{B}(Ca_{1.84}Na_{0.16})^{C}(Al_{0.45}Ti_{0.08}Fe^{3+}{}_{1.22}Mg_{0.53}Fe^{2+}{}_{2.44}Mn_{0.07})_{\Sigma=4.78}{}^{T}(Si_{6.13}{}^{IV}Al_{1.87})O_{22}{}^{W}(OH_{1.70}F_{0.30})$$

The occurrence of potassium-dominant amphiboles is rare has been reported in K-rich igneous rocks and their affiliated metasomatism (Mazdab, 2003). Potassichastingsite from igneous origin is only reported from evolved peralkaline granites or syenites, but the most frequent origin is metasomatic. Fluorine was determined qualitatively only due to the high Fe content, and hence the OH/(OH,F) is only indicative. The LOI corrected for Fe^{2+} indicates H_2O is present dominantly in the formula.

Ilmenite is a rare mineral in the rock and all crystals are rimmed by titanite or REE fluorocarbonates. They probably are relict from the pre-metasomatic rock assemblage. The compositions are plotted on the Fig. 14f in the ternary hematite-ilmenite-pyrophanite. The calculated average composition is Hem10-Pyr10-Ilm80. Ilmenite contains some inclusions of fergusonite-(Y) as determined by EDS scans.

Apatite is abundant in the rock, as large millimetre-size anhedral grains or smaller crystal aggregates. All apatite are fluorine-rich (fluorapatite). The composition is Y-rich, showing up to 2.5 Wt-% Y_2O_3. The increase in Y is directly correlated to Si, which substitute P. This non stoichiometric exchange tends toward the britholite-(Y) end-member: $(Y,REE,Ca)_5(SiO_4,PO_4)_3(OH,F)$ (Fig. 15a &b). It seems two populations of fluorapatite are present, a Y-poor and an Y-rich and Si-bearing populations.

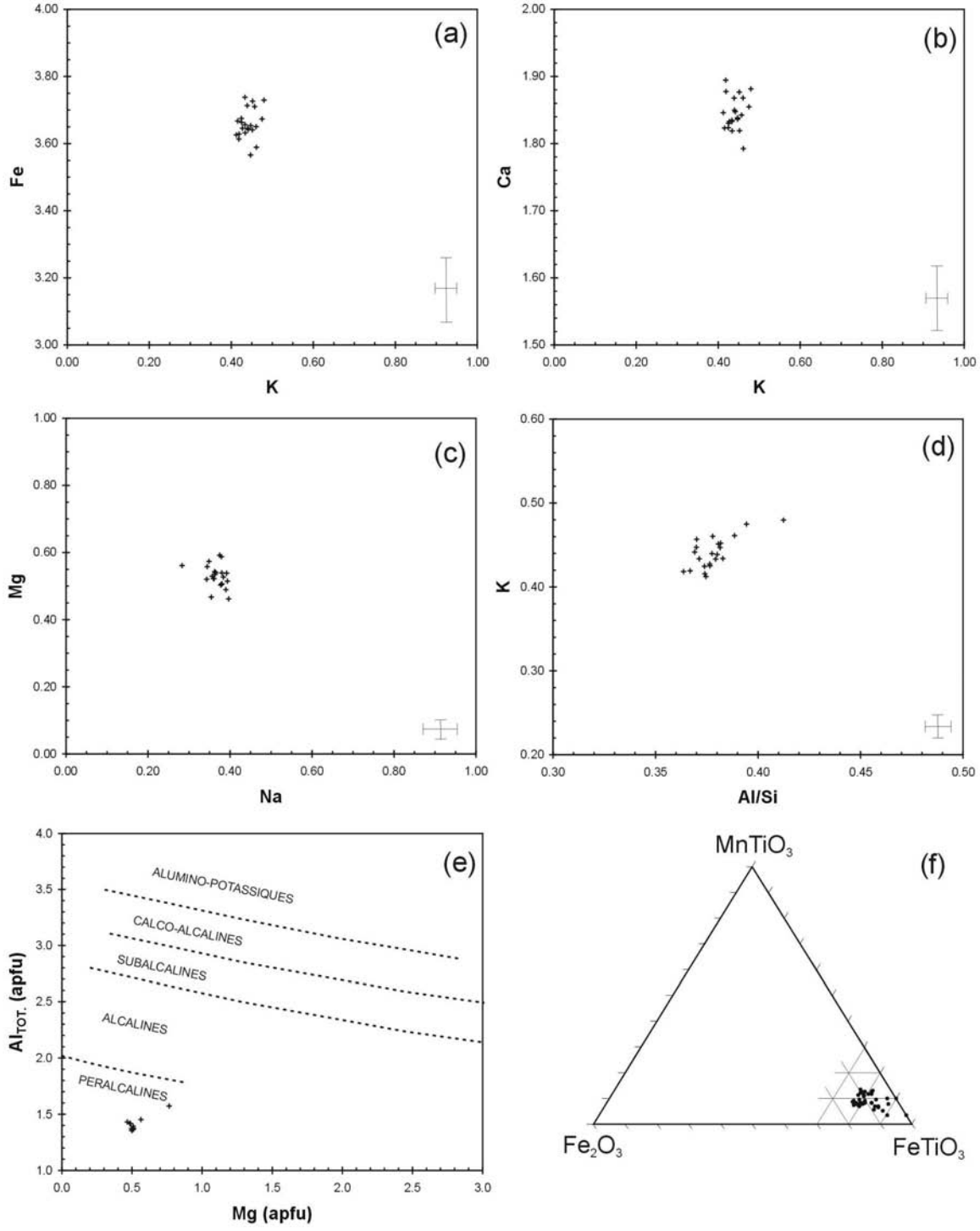

Fig. 14: Chemical representation for amphibole, biotite and ilmenite from YER-03

(a,b,c,d) The amphibole is a potassic-hastingsite, with a solid solution toward a ferro-tchermakite or ferro-ferri-tchermakite; the reported analyses lie in the incertitude of each other, meaning the mineral composition is homogenous. A minor variation is only recorded for the Al/Si ratio; (e) biotite composition is Fe-rich, close to the annite end-member; it plots in the field of the peralkaline or alkaline granite suites (A-type) defined by Nachit et al. (1985); (f) ternary hematite-ilmenite-pyrophanite.

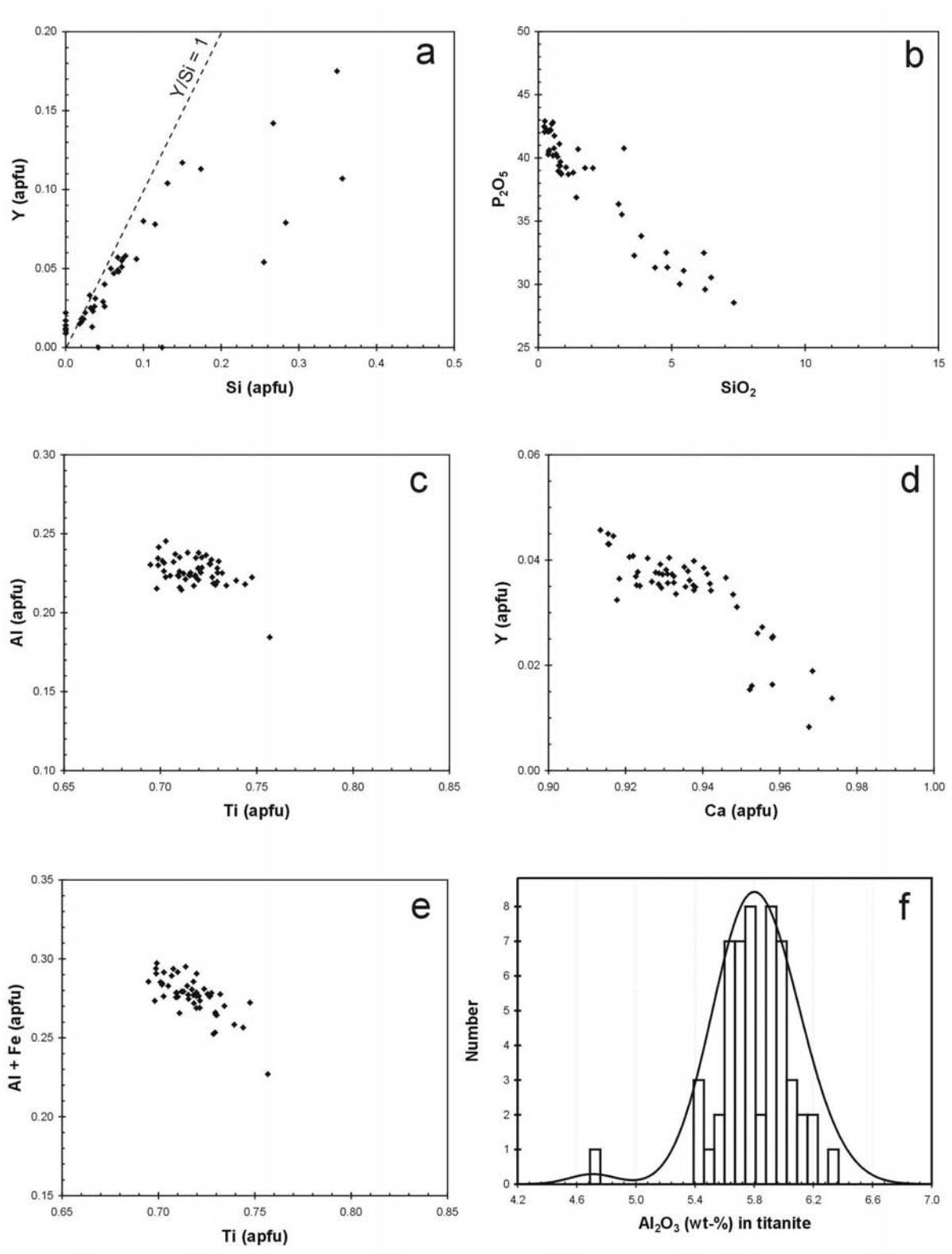

Fig. 15: Chemical representation for apatite and titanite from YER-03

(a) Y versus Si in fluorapatite: the two elements are correlated and evidence the britholite substitution; (b) P_2O_5/SiO_2 in fluorapatite: the increase in Si is counterbalanced by a decrease in P; (c)(d)(e)(f)The titanite in Yerila is REE and Y-rich. The introduction of Y, REE occurs in the Ca position and operates the $[Ca]_{-1}[Y+\square]_{1}$; (e) Ti is also substituted by Al and Fe^{3+}; (f) the distribution of Al in titanite is regular, following a Gaussian curve centred at 5.8 Wt-% Al_2O_3.

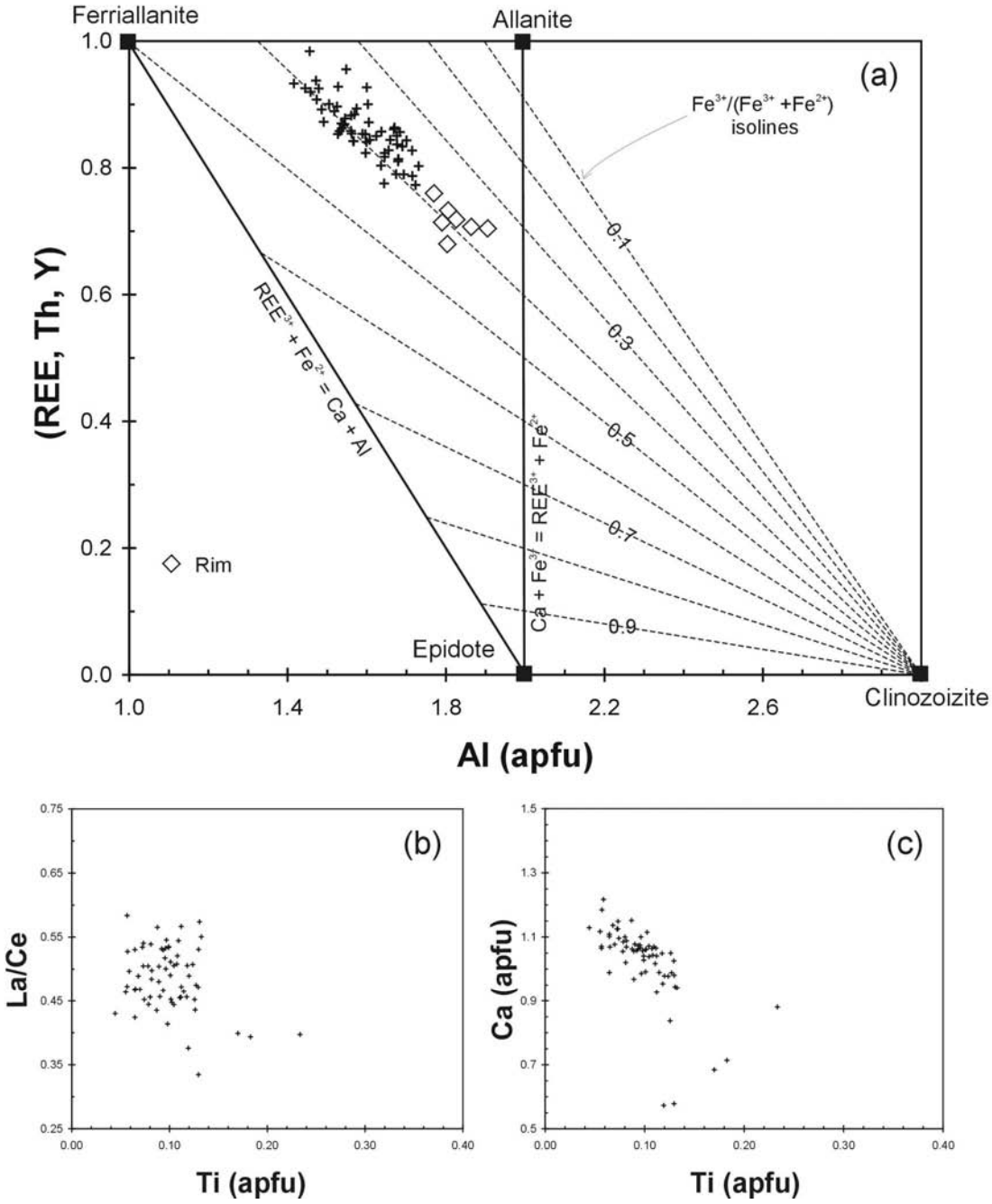

Fig. 16: Chemical Chemistry of allanite in Yerila (YER-03)

(a) Diamond symbols represent allanite rim compositions; the allanite substitution relations are illustrated in the diagram from (Petrik et al., 1995). The sorosilicates end-member of the epidote group are forming the corners of the diagram and theoretical $Fe^{3+}/(Fe^{ToT})$ isolines are drawn from clinozoizite (Fe-free). The values for Yerila plot along the 0.35 and 0.42 isolines; (b) La/Ce is clustered around 0.50, all points are within the error of each other. The altered allanite have lower La/Ce ratio, and higher TiO_2 content; (c) the highest TiO_2 contents, apart from the weathered allanite, are correlated with the lower Ca (high REE) from the allanite cores.

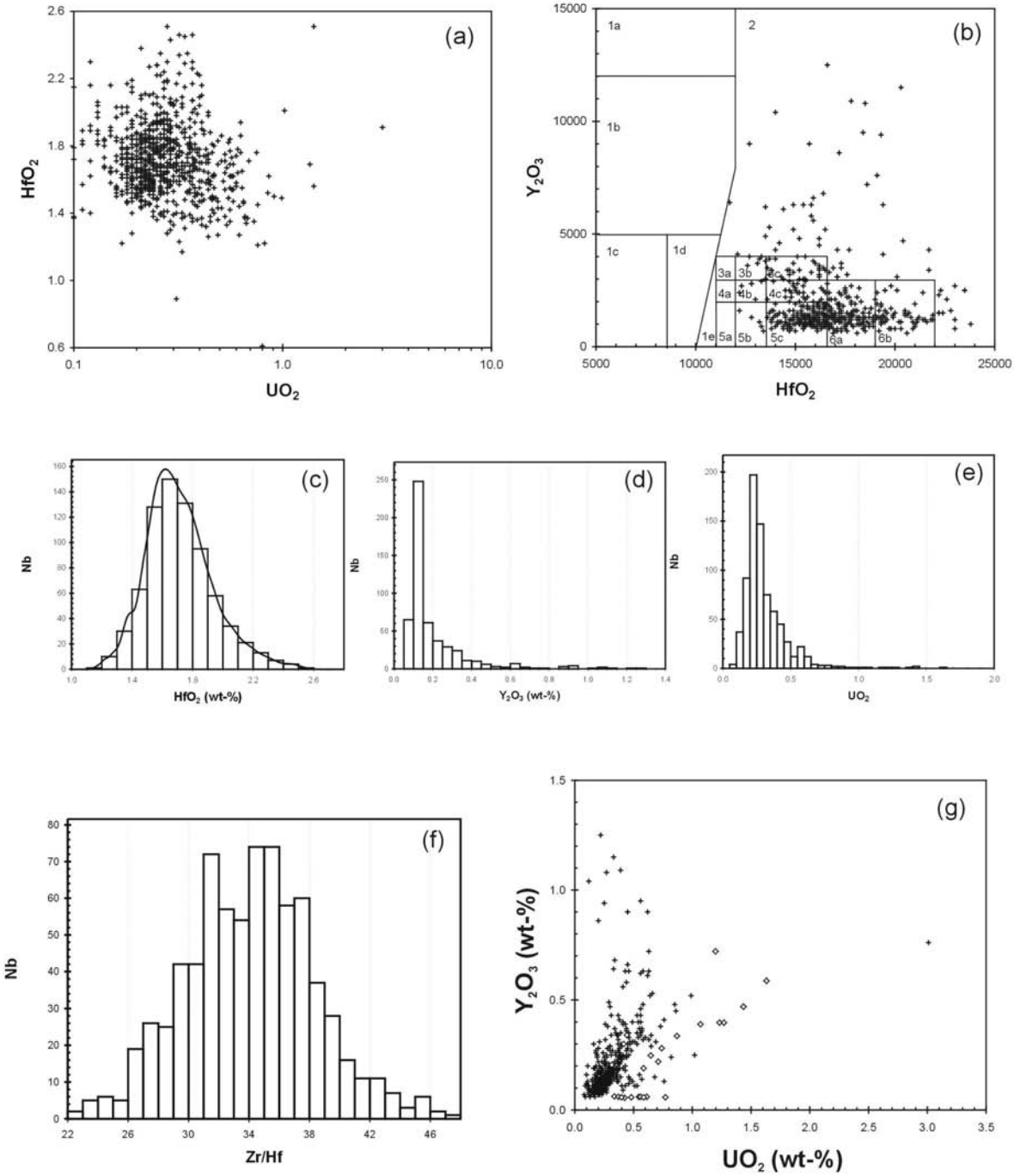

Fig. 17: Chemical representation for zircon from YER-03

700 analyses by electron microprobe have been used in the diagrams. (a) HfO_2-UO_2 diagram illustrates the U-rich composition of zircon (median value 0.28 Wt-% UO_2); (b) The Y_2O_3-HfO_2 diagram with proposed geodynamics discrimination boundaries for granitoids (Pupin 2000); the analysed zircon are all magmatic or late magmatic. The distribution of the points clearly evidences the total absence of Hf-poor zircons. Zircons from anorogenic rocks with only mantle or mainly mantle origins bear Hf contents <11000 ppm HfO_2 (zones 1a to 1e). The higher 14000-20000 ppm HfO_2 suggests a crustal origin (anatectic crustal granites, migmatites) or alkaline subsolvus magmas. (c) to (f) distribution histograms for HfO_2, Y_2O_3, UO_2 and Zr/Hf; note the detection limits (d.l.) for Y_2O_3: 0.06 % and UO_2: 0.08%; around 25% of zircons had Y below d.l. whereas U was always over d.l. This is visible on (g).

Titanite is the also showing a unusual composition with high Y and REE content (up to 2.5 Wt-% Y_2O_3), as well as moderate Al_2O_3 and Fe_2O_3 (5.8 and 1.6 Wt-% in average; Fig. 15c-d). The fluorine content is high (>2 Wt-%). The presence of Al, Fe^{3+} and REE is the result of combined substitutions under oxidized fluorine-bearing fluids. The "grothite" substitution $(REE)Fe^{3+}Ca_{-1}Ti_{-1}$ and the (Al,Fe^{3+}) <-> Ti^{4+} + $(OH,F)^-$ can both be found. The aluminium which enters in the titanite structure has been linked to a high-pressure genesis (Tropper *et al.*, 2002). However, the moderate substitution found (0.20-0.25 Al apfu) and association with fluorite suggests titanite formed at low to moderate pressure and high temperature (<6 kbar; >400°C). Despite P-T diagrams were only poorly calibrated in the low-P range, the compositional ranges of synthetised titanite at definite temperatures indicates Yerila compositions most likely correspond to high-level (<6kbar), late-magmatic to post-magmatic conditions (Tropper *et al.* 2002). The presence of Y (REE) substitution in these Al-F-rich titanites also records the mobility of these elements during this metasomatic stage.

Allanite is a common accessory mineral whose size reaches five millimetres. Its composition corresponds to an intermediate between allanite-(Ce) and ferriallanite-(Ce) (Fig. 16a). Some of the crystals are rimmed by epidote-clinozoizite. Allanite has nearly constant thorium content around 1 Wt-% ThO_2. In contrast, MgO and TiO_2 decrease simultaneously when pointing to the clinozoizite end-member. Small inclusions of fluorite, uraninite, thorite, zircon and apatite are scattered in allanite. A special study of the zircons included in allanite is presented after. Most allanites appear isotropic in the thin sections indicating a metamict state. This has also been confirmed by X-ray diffraction. La/Ce is clustered around 0.50; all points are within the error of each other. The altered allanite have lower La/Ce ratio, and higher TiO_2. The calculated average structural formula is:

$$(Ca_{1.03}Ce_{0.47}La_{0.22}REE_{0.24}Y_{0.02}Th_{0.02})_{\Sigma=2}(Al_{1.55}Fe^{3+}_{0.50})_{\Sigma=2.05}(Fe^{2+}_{0.68}Ti_{0.09}Mg_{0.04}Mn_{0.03})_{\Sigma=0.84}Si_3O_{12}(OH,F).$$

Many small uraninite crystals are widespread in the rock, mostly as mineral inclusions (e.g. in zircon and allanite). We only analysed one large inclusion (150 μm) in a zircon; this uraninite also contains Zr, Th, Y, REE, Pb and Si in percents. A Th-U-Pb age calculation on the chemical analysis gives an indicative age of 491 Ma.

Molybdenite is a trace mineral in the rock, generally associated with biotite or located at the main minerals boundaries. Most grains are showing a powellite rim. Molybdenite chemistry was investigated by EDS only. The composition is pure MoS_2, and no Re was detected (Re < 0.5%).

REE-fluorocarbonates are scattered throughout the Yerila granite, as a late phase, essentially occurring in the biotite layering of the gneiss. Light creamy brown patches reaches 2-3 millimetres and are frequently mixed with thorite and contain relicts of ilmenite. The microprobe analyses are all normalized on five cations; fluorine has been precisely determined due to the minimal content of iron. The calculated ideal formula after deduction of Al and Si content is: $Ca(Ce_{2.22}La_{1.15}Nd_{0.47}Y_{0.08}Th_{0.06})_{\Sigma=4}(CO_3)_5F_4$ This formula indicates a mineral composition which is a intermediate in the synchysite-(Ce), parisite-(Ce), röntgenite-(Ce) group.

Additional minerals were also analysed:

- Euxenite-(Y) as an inclusion in ilmenite: $(Y_{0.74}Fe_{0.04}Ca_{0.02}Yb_{0.10}U_{0.09})_{\Sigma=1}(Nb_{1.95}Ti_{0.05})_{\Sigma=2}O_6$
- Chevkinite-group mineral present in the fluorocarbonates aggregates: $(Ce_{2.81}La_{0.05}Ca_{0.30}Th_{0.10}U_{0.07})_{\Sigma=3.33}(Ti_{1.34}Fe^{3+}_{0.21}Zr_{0.02}Mg_{0.04}Al_{0.22})_{\Sigma=1.83}.(SiO_4)_2O_4(OH,F)_2$
- Thorite-Coffinite solid solution minerals [2.8 – 22.6 -% UO_2, 0.2-7.0 Wt-% Y_2O_3]

The whole-rock and mineral separates chemical composition are reported in the Appendix III. The SiO_2 content of YER03 is 65.7% placing the granitoid in the intermediate rocks category. The rock fits into the field of the monzogranites under the De La Roche classification R1 = 2053, R2 = 572 (De La Roche et al. 1980). However, other samples of Yerila are a lot more felsic (YER5) with 75% SiO_2 and correspond to a granite composition.

The CIPW composition of Yerila gives the following virtual assemblage: apatite 0.3%, ilmenite 0.2%, orthose 34.9%, albite 18.4%, anorthite 9.8%, titanite 1.1%, hematite 6.1%, CaO –diopside 0.1%, MgO –diopside 0.1%, CaO-SiO2 wollastonite 0.7%, hypersthene 1.9%, quartz 24.2%. The corresponding QAPF indices are 24.2, 34.9, 28.2 respectively (%-normative) and 27.8, 39.9, 32.3 (%-relative). It enters the field of the granite under the Streckeisen classification. The agpaïtic index = 0.736. $(Al_2O_3 + CaO)/(FeO^{tot} + Na_2O + K_2O)$= 1.18. $100*((Mg+FeO^{tot} +TiO_2)/SiO_2)$ =10.48. The composition is slightly peraluminous with an ASI index of 1.11.

The composition is especially enriched in HFSE, Zr in particular. However, due to the abundance of fluorine in the rock, the overall behaviour of commonly "immobile" elements is modified, making trace elements geochemistry mostly inapplicable. This behaviour also applies to Fe, with biotite having crystallised late in the sequence. Pure biotite separates were analysed separately and display the strongest enrichments in HFSE due to late stage HFSE inclusions.

SED-BAD / AMPH9:

The garnets were analysed by EMP and results are reported in Figure 18. Nearly all compositions are along the solid solution Almandine-Spessartine, generally between $Alm_{55}Spes_{45}$ and $Alm_{70}Spes_{30}$. Other compositions are near pure Almandine (Alm_{94-97}) or Spessartine ($Alm_{34}Spes_{66}$). Overall, garnet compositions are compatible with garnet-bearing peraluminous granites. The mineral was locally observed in some granite pegmatites spreading around the close-by Mudnawatana intrusion.

Monazite compositions were measured by EMP and dated using total U-Th-Pb. The compositions are all monazite-(Ce), with generally high ThO_2 content varying between 2.5 and 10 Wt-%. The monazites are generally low in Ca and compositions lie on the solid solution huttonite-monazite ($ThSiO_4$-$REEPO_4$) (Fig. 19). The presence of monazite rather than allanite also indicates that the local Yerila granite averages peraluminous compositions; monazite is antinomic of allanite. This has especially implications for the Th and U distribution. The average Th/U ratio of the monazite in SED-BAD is 32. Xenotime is less frequent than monazite and the visual distinction of these two yellow-coloured minerals requires experience; the xenotime shows a yellow pale colour and sometimes a greenish nuance. Its composition was checked by SEM and the only quantitative data are U and Th, obtained by the LA-ICPMS dating. Th and U compositions of xenotime are reported on Figure 19.

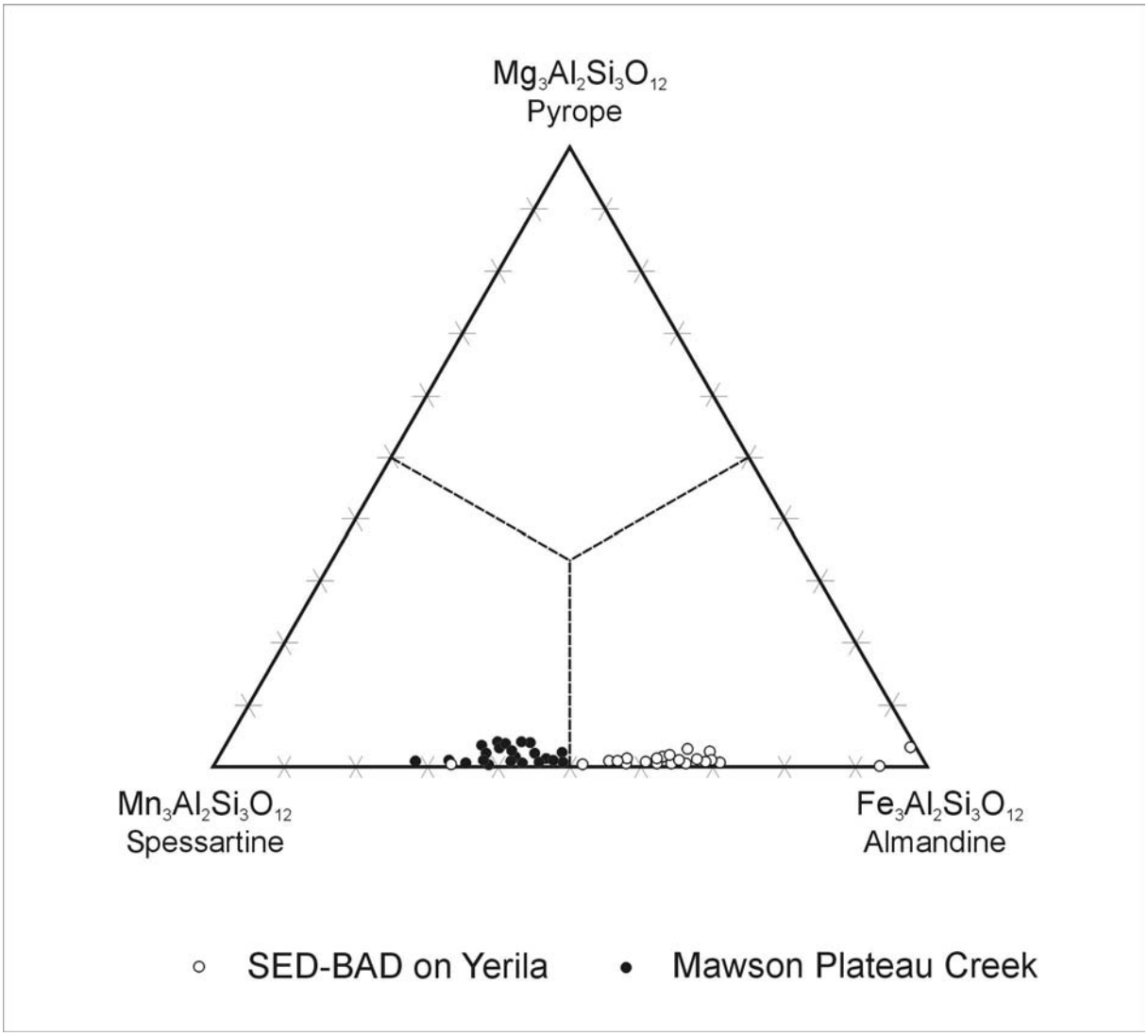

Fig. 18: Ternary diagrams for garnets from SED-BAD and SED1 samples

The garnets from both localities all fit in the pyralspite solid solution and correspond to the compositions of garnets from peraluminous granites. The coarse grain size of many of them also indicates their origin is pegmatitic.

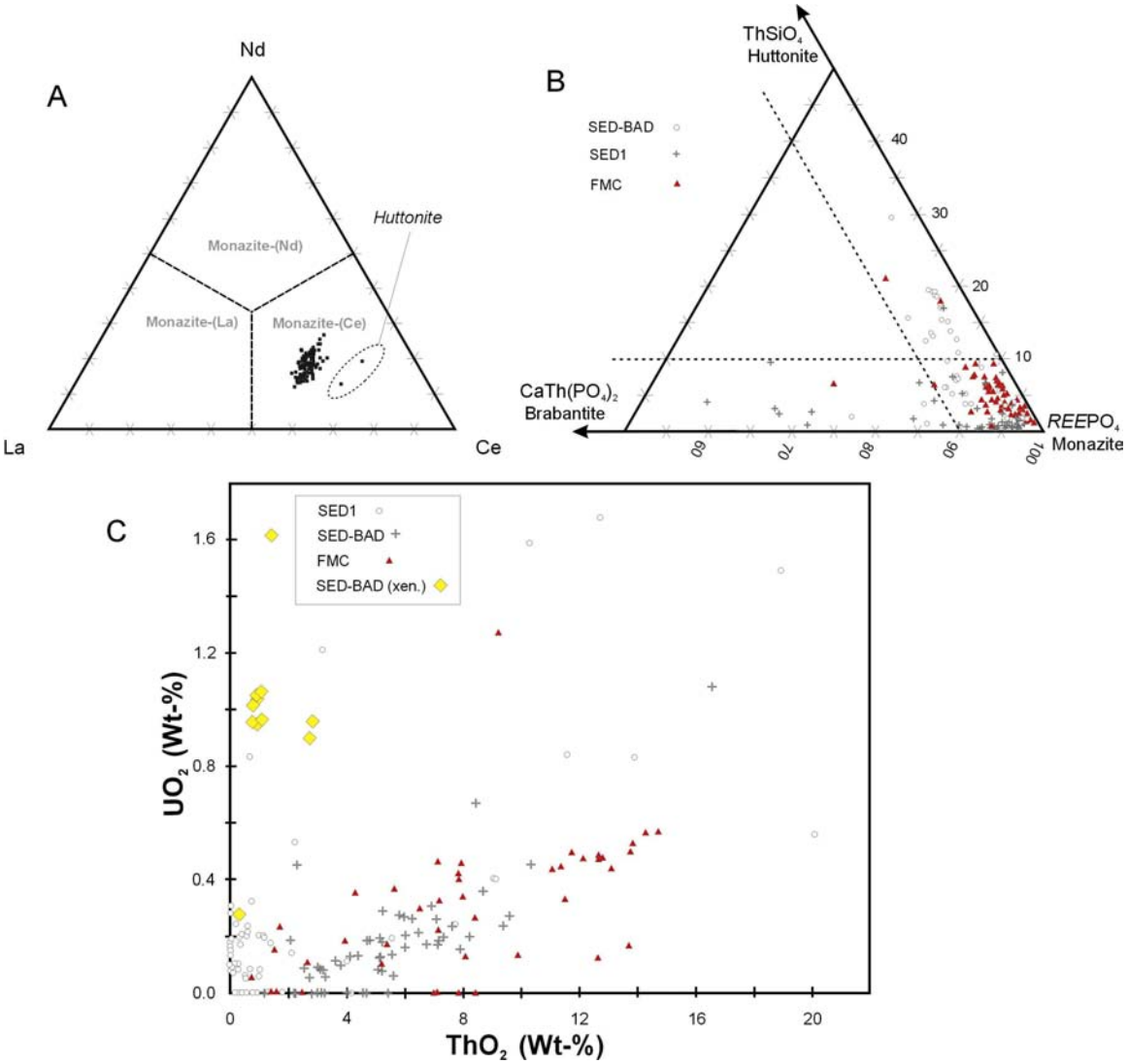

Fig. 19: Monazite and xenotime chemistry diagrams from SED1, SED-BAD and FMC

(A) All monazite fit in the monazite-(Ce) field, Nd- or La-rich monazites are unusual and generally related to hydrothermal or alteration processes; (B) the solid solution huttonite-monazite-brabantite shows the presence of several populations: a dominantly huttonite-monazite trail of composition for FMC and SED-BAD (biotite gneisses origin) and a brabantite-monazite trail for SED1 (peraluminous muscovite granite and pegmatite); (C) the UO_2-ThO_2 diagram also represents a few xenotime-(Y) from SED-BAD; the SED1 monazites (brabantite-monazite solid solution) are relatively poor in ThO_2 for and equal quantity of UO_2, compared to SED-BAD and FMC, this generally reflects the unusually low Th/U ratio (~1.0) of the British Empire granite.

The rare minerals from SED-BAD, Yerila-Ck or AMPH9 were essentially identified using by semi-quantitative SEM analyses (EDS). The presence of rare, Ce-rich minerals has important consequences for the origin of REE-Th-U in the Yerila granite (Table 3). The presence of REE-bearing compositions with "Cerium only" is certainly due to oxidation and Ce^{4+} concentration or immobilisation in them. The presence of cerium IV is not rare in supergene environments and the photos on the Figure 20 illustrate well the secondary origin of these minerals. In comparison to the REE mineralogy described in the YER-03 sample, additional species are recorded here, especially because the sedimentary sample represents a much representative regional sample fluocerite-(Ce) was found in the sample and certainly represent a primary late-magmatic mineral. The presence of this mineral is generally restricted to peralkaline granites. In the present case, metasomatism is probably involved since no rocks of this type occur in the watershed.

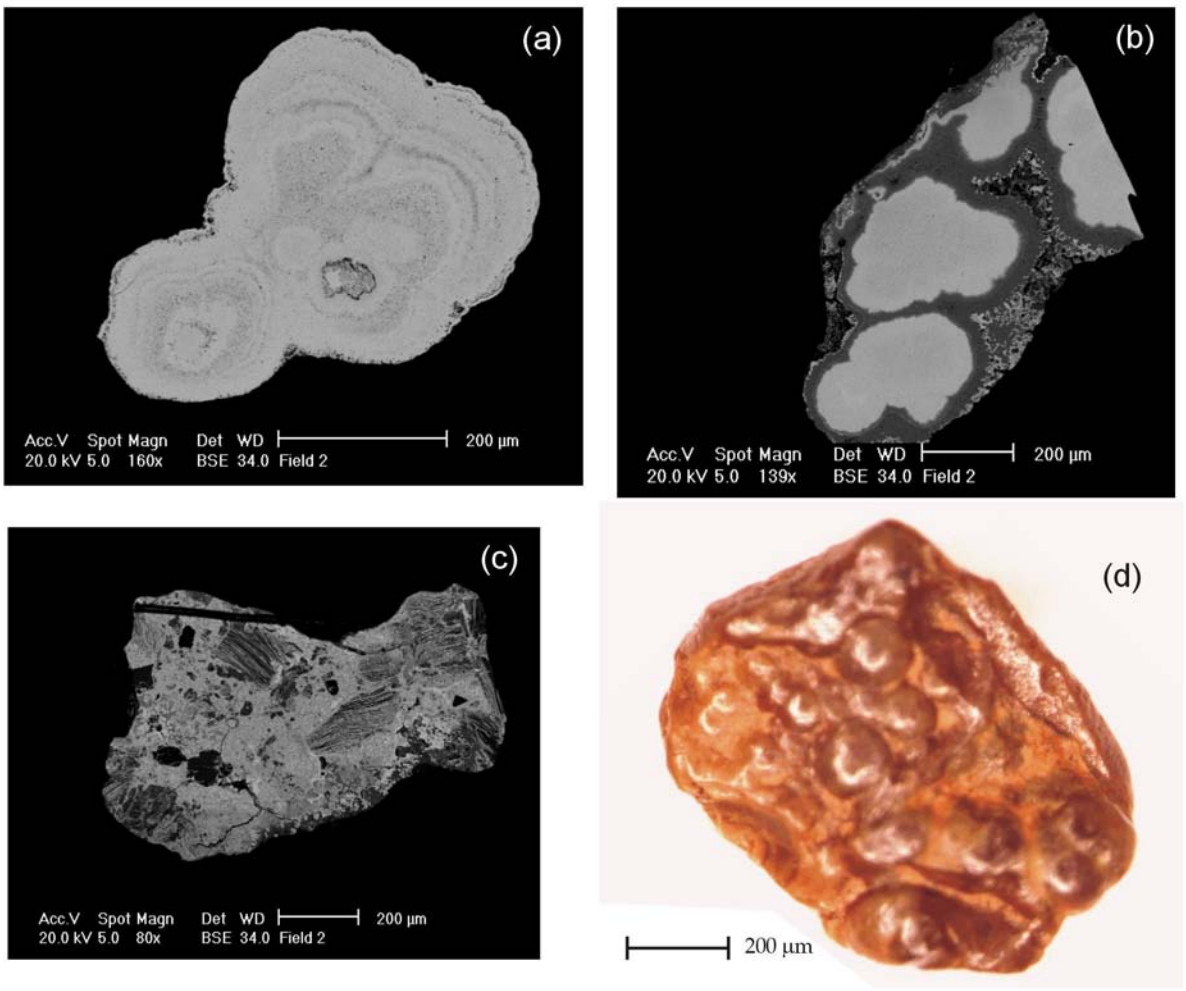

Fig. 20: Cerianite and cerium-rich hollandite group grains from SED-BAD

(a) (b) BSE image of cerianite grains with a supergene reniform shape; the mineral composition gives more than 90 Wt-% CeO_2, with minor Si, Ca and Mn; (c) Pb-rich and Ce-rich hollandite-type grain with exfoliated micas cemented; oxidation of both Mn and Ce are required to produce this aggregate; (d) coloured picture of the previous grain prior mounting and polishing. The possible precursor mineral to cerianite is probably a REE-fluorocarbonate (synchysite, bastnäsite, etc.) or the mineral fluocerite (Ce,La)F_3.

4.2 The allanite skarns from the Brindana Gorge area

The recent radiometric survey on the MPD brought to light an area to the South of the Brindana Gorge, characterised by high-Th and high-U counts. The recent geology investigations (Sheard and Callen, 2000) and (Stewart and Foden, 2001) lead to a redefining of this zone previously mapped as "granitised metasediments, quartzites and hornfels skarns" (Campana et al. 1961), and then partly regrouped into the more general "Brindana schists" formation (Coats & Blissett, 1971; Fig. 3). The radiometric anomaly is considered as an equivalent to the "Yerila granite" by Stewart & Foden (2001), on the basis of the geochemical signature of some of the samples. More subdivisions occur on the 2000 map (Fig. 21); the zone is split into an undifferentiated granitoid (presumably Mesoproterozoic), quartzites, minor Box Bore orthogneiss, and the Brindana schists. Skarns and hornfels are mapped individually on the 1961 maps and our investigations focused on these horizons whose primary origin was undoubtedly recognised as sedimentary by all workers. The location is reported on a new scaled map (Fig. 21), with the recent subdivisions of Sheard & Callen (2000), with the anomaly defined as a separate "Yerila-type unit" by Stewart & Foden (2001) and the original hornfels-skarns mapped by Campana et al. (1961a). During the review of the exploration data and the whole-rock analyses available on the PIRSA database, it appeared that the high-Th-U-REE values occur accross all of the petrological subdivisions recognised by Sheard & Callen (2000); for this reason, the origin of the radiometric anomaly could not be related to a specific intrusion only. The possibility of a Th-U-REE metasomatism was adopted as a starting hypothesis and this localized study on the hornfels skarns at the edge of the anomaly aims to document this eventuality. Two samples close to each other were obtained at the Southern border of the anomaly, on the thin skarn horizon mapped by Campana et al. (1961a): JB05-36 & 37. Additionally, the entire anomaly was walked across from north to south.

JB05-36

The sample is a dense grey gneiss containing 2-3 mm porphyroblasts of allanite. At a larger scale, some veinlets can be observed, magnetite- and allanite-bearing, giving a dark brown colour to some of the cracks. The main minerals are quartz, feldspar, hastingsite. The texture is medium-grained, with an equigranular distribution. Hastingsite appears as subparallel laths and porphyroblasts, associated with granular anhedral titanite and fine magnetite. Hastingsite has a preferred orientation. Allanite forms 100 µm to 5 mm crystals associated with minor epidote; the mineral is younger and replacive. Other accessory minerals are zircon and apatite. The composition of the rock present similarities to the Yerila granite in regard to HFSE: 800 ppm Zr, 320 ppm Y, 86 ppm U, 385 ppm Th, 1250 ppm Ce and 6.8 ppm Ta.

JB05-37

The second sample comes from a dark massive outcrop forming a prominent spur in the landscape. It consists of a hornblende hornfels, composed of scattered hastingsite crystals in a fine-grained matrix of quartz, microcline and minor chloritised biotite. Allanite is abundant (2-5 %) and forms patches up to 8 mm in size. Fine-grained magnetite is widespread through the rock. Other accessories are titanite, zircon, fluorapatite, and minor amount of a yellow Th-rich silicate mineral, fluorite and pyrite. Allanite is porphyroblastic and seems to be replacing earlier epidote, or is intergrown with contemporary epidote. Larger crystals of hastingsite are porphyroblastic. The rock is interpreted as a type of skarn, in which a quartzo-feldspathic metasediment was metasomatized with formation of hastingsite, allanite-epidote and titanite and deposition of magnetite. Because of the high proportion of introduced minerals, the geochemistry of the rock certainly reflects closely the chemistry of the metasomatism.

Heavy mineral separates were examined in detail and the zircon typology characterized. Zircon is light brown in colour and the "D-type" only was recognised. Small amount of a very dark, almost black rutile was identified. It forms small crystals or twins. Most grains are xenomorphic. Because of its rounded shape, rutile may have a detrital origin. The rock chemical composition is extremely rich in Th (515 ppm), Y, Nb, Zr, U (220 ppm) and REE. The rock is calcic (4.70 Wt-% CaO) in relation to hastingsite. Comparing the HFSE, in Yerila and JB05-36-37, a immediate similarity appears. Since the rock has a clear sedimentary origin, the metasomatic overprint is well recorded, without the interference problem of other granitic rocks. The following geochemical signature can be established for the metasomatism: Ce-Zr-Th-Y- La-Nd-U-Nb-Ta.

Northern calcsilicate layer and other rocks in anomaly

The nature of the "skarn-hornfels" layer to the north was confirmed to be identical to the sample JB05-39. Magnetite, diopside, hastingsite and allanite form the chief minerals. Observations made on the N-S profile of the anomaly are surprising. Only one type of rock was observed and consists of red gneiss with leopard-like centimetric biotite eyes. The gneiss is rich in pink K-feldspar and also bears quartz, biotite and zircon. The radioactivity on the profile invariably sits around 2000-3000 cps on SPP2, indicating the rock is quite homogenous. These observations are contradictory to the recently published data (Sheard & Callen, 2000) and favour the 1961 observations.

The nature of these gneisses should be investigated in detail with additional data on their zircons to solve the question of their origin. Ultimately, the map necessitates an entire revision at an appropriate scale.

4.2.1 Mineral chemistry

The mineral chemistry of the samples was not studied in detail and the focus was directed to the geochronology. The "yellow Th-rich" mineral was investigated by SEM and its chemical composition is discussed here.

Several grains were analysed by EDS and Th, Si, U and Ca were detected. The semi-quantitative composition was calculated for the two extreme compositions met on the basis of four oxygen anions: $Th_{0.42}Ca_{0.35}U_{0.19}Si_{1.24}O_4$, and $Th_{0.66}U_{0.21}Ca_{0.02}Si_{1.12}O_4$. The electron beam of the microscope damaged the surface of the mineral, which is a common phenomenon met when analysing hydrated minerals. For this reason, we consider the mineral to be a hydrated calcium-rich thorite. Rutile was analysed by LA-ICPMS for geochronology purpose. Its uranium content is extraordinarily regular and stays close to a value of 130-140 ppm U, this with Th under the detection limits. We can refer to it as a uranium-rich rutile.

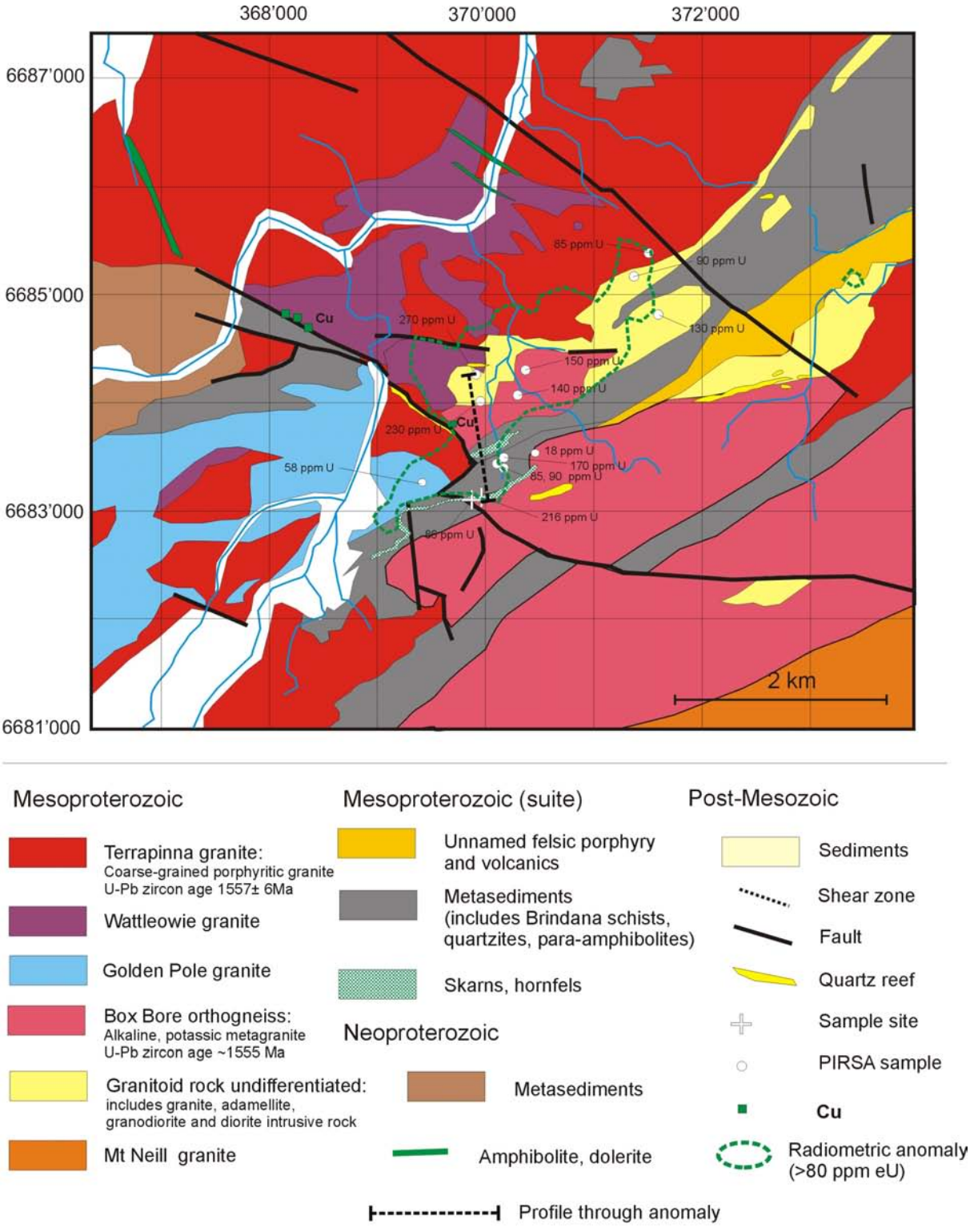

Fig. 21: Geological map of the Brindana Gorge and the radiometric "Yerila-like" anomaly

The geological map was prepared using the 1961, 1971, 2000 maps and also some unpublished data available on the PIRSA database. The metasediments have been simplified for the purpose of this study, only underlining the hornfels and skarns distinguished on the 1961 map. The area is located around 12 km to the South of Mount Babbage, to the east of Mt Fitton Station. A walked profile indicated on the map showed a continuous succession of red gneisses with eyes of biotites (leopard-style) with high radioactivity (2000-3000 cps on SRAT SPP2 scale). The two hornfels/skarns layers on the map are Ca-rich metasomatised sediments of identical nature with chiefly diopside, allanite and magnetite. These limited observations indicate most of the reported geology is certainly erroneous!

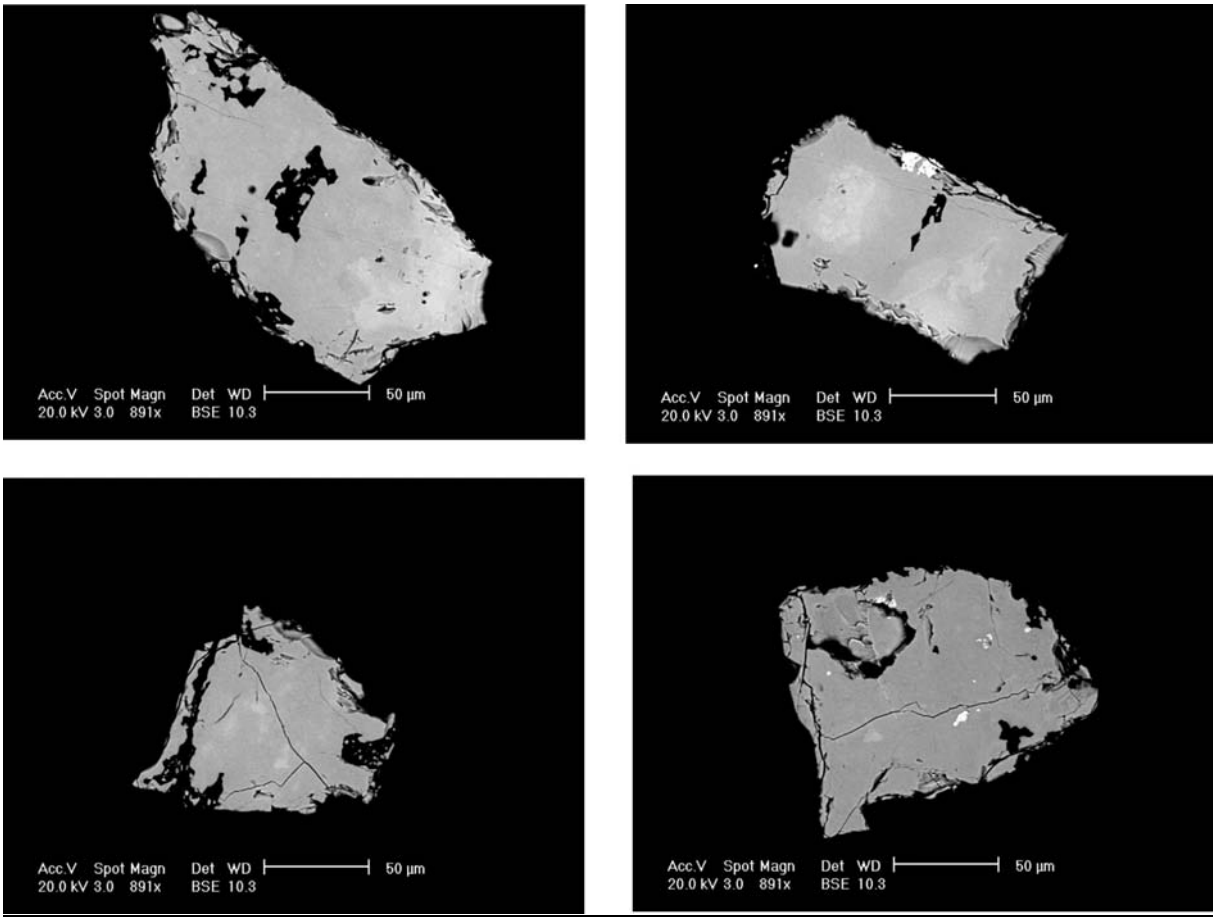

Fig. 22: Th-U-Ca silicate grains from the skarn JB05-37

The zoning in the grains is probably related to hydration but also to the concentration of (Th + U) versus Ca. Small bright inclusions of uraninite are visible. The nature of the cracks suggests the mineral to be metamict.

4.3 The Mawson Plateau watershed

The investigations carried on the Mawson Plateau have been of very limited extend. A day expedition was led to the central plateau to sample the main creek alluvium (Sample no. SED1). Several leucogranite and pegmatites samples complete the dataset.

The Mawson Plateau is entirely cut in the British Empire Granite (BEG) and the Freeling Heights Quartzite, forming a basin pan drained by a single outlet ultimately joining the Hamilton Creek, near the Terrapinna Waterhole. The granite has been divided into a major S-type peraluminous granite body with a minor I-type granite tail on its SE extremity (Elburg *et al.*, 2003). This distinctive part is now regrouped in the Paralana Granodiorite as defined by Stewart & Foden (2001). The mineralogy of the I-type as reported by Elburg *et al.* (2003) consists of oligoclase, K-feldspar, quartz, biotite, with minor muscovite. The accessories are apatite, zircon, monazite and titanite. The S-type lacks biotite, and contains a lot more K-feldspar. Biotite occurs in schlieren next to the edge of the intrusion or its migmatitised transitional contact to the Paleoproterozoic metasediments (McLaren *et al.* 2006). The radiometric signature is clearly potassium dominant and the Th/U ratio averages ~ 0.5-1.0. The S-type granite is coarse and frequently grades into garnet-bearing pegmatites. Monazites from both S- and I-types have been dated by U-Pb and give an age range from 444 to 441 Ma ($^{207}Pb/^{206}Pb$ isochrones) (Elburg *et al.* 2003). Large garnet from pegmatitic granite have given $^{207}Pb/^{206}Pb$ 447.8 +7.1/-3.4 Ma whereas monazites give a weighted average of $^{238}U/^{206}Pb$ age of 442.7 ± 8.2 Ma (McLaren *et al.*, 2006). Most of the zircons from the BEG are inherited and only two concordant crystals with ages between 440 and 460 Ma are mentioned in McLaren *et al.* (2006). Pegmatite with garnet, muscovite and beryl were observed on the Mawson Plateau.

4.3.1 Mineralogy

SED1

The sample SED1 was collected in a natural fissure in the bedrock of the main creek, just a few meters before a waterfall. The HM's contain a group of large (1-5 mm) minerals: red garnet, yellow monazite, xenotime, black tourmaline and rutile a population of finer minerals: magnetite, ilmenite, garnet, monazite, rutile, xenotime, columbite, white zircon, apatite, titanite, very angular corundum, limonite and beryl.

JB05-19

The sample consists of a muscovite coarse-grained alkali leucogranite. The main minerals are subhedral grains of quartz, microcline and subordinate cloudy albite. A minor proportion of muscovite and very little biotite are present. Accessory mineral is apatite. The trace element chemistry of JB05-19 is typical from the S-type intrusion with very low Zr (43 ppm), REE (13 ppm Ce). The most interesting character is U (17 ppm) and a U/Th ratio =1.9.

4.3.2 Mineral chemistry

The composition of garnet was determined by EMP on the coarse grains from the sample SED1, garnets interpreted to be of pegmatitic origin, as observed on the outcrops several times. The compositions range from $Alm_{27}Spes_{73}$ to $Alm_{48}Spes_{50}$, with pyrope content between 0 and 5%. The compositions are reported on the ternary diagram Pyrope-Almandine-Spessartine (Fig. 18). Spessartine is a common mineral in peraluminous granites, and its presence in British Empire Granite is normal.

Monazite from the Mawson plateau has been also analysed by EMP and dated using the same technique, measuring Pb, Th and U. The compositions range from nearly pure monazite-(Ce) and follow a trend towards the brabantite pole ($CaTh(PO_4)_2$); the extreme composition met is: Mon-57%-Bra-38%-Hut-5%. The Th/U ratio of most of the monazite is unusually low (< 12) and many crystals had Th below detection limits (Fig. 19).

4.4 Mt Gee - Radium Ridge area mineralisations

The region of Mount Painter, Mount Gee and Radium Ridge has not been the main interest of this thesis. However, a limited amount of work was directed on U-Th geochronology of the uranium primary mineral species found in this area. Two localities were selected: (1) Radium Ridge, Number 2 Workings where some uranium-niobium minerals occur and (2) the Number 10 Workings, an almost lost locality described for the last time by Mawson in 1944 and hosting a "radioactive ilmenite". Heavy mineral concentrates from regolith also complete the data on this area.

4.4.1 The hematite-monazite bodies at Radium Ridge Nr.2 Workings

The No. 2 deposit of Radium Ridge mineralisations group is located on the northern slope of the ridge. The lens outcrops on approximately 20 x 5 m. No more than 15 m separate the No.2 body from the No.1 workings (similar sized body 15 x 5 m). The orebody consists of a small lens of hematite, quartz and monazite-(Ce). These are the major minerals but numerous other minor minerals have been recorded in the early studies (fergusonite-samarskite, uranosphaerite, torbernite, metatorbernite, uranophane, and gummite) (Brugger et al. 2003; Coats and Blissett, 1971).

Recent mineralogical investigations by workers at the South Australian Museum have lead to the discovery of new mineral species and a more detailed paragenesis has been described. The following minerals are recorded: hematite, quartz, monazite-(Ce), xenotime-(Y), a Fe-Nb-U-rich euxenite-group metamict mineral (samarskite-fergusonite from early descriptions), fluorapatite, a Fe-phosphate hydrated (phosphosiderite?). A primary prismatic U mineral is altered into a mixture of soddyite, beta-uranophane, billietite, schoepite, and metaschoepite, rutherfordine and spriggite. Additionally are also described the secondary following minerals: kasolite, Ce-rich françoisite-(Nd), metatorbernite, Ba-bearing boltwoodite, weeksite and barite.

The ore can be described as a Fe-REE-U ore. I analysed a typical monazite-(Ce)-bearing ore sample using XRF (Table 4). The whole-rock composition underlines the absence of feldspars or any alumino-silicates. The REE_2O_3 and P_2O_5 molar-% are close to each others and this confirms the REE are entirely hosted by monazite-(Ce) and/or xenotime-(Y).

The age of the hematite orebody has been investigated by (Kleeman, 1946) on "samarskite" and his 400 Ma age can be recalculated to 394 ± 38 Ma, using the current uranium decay constants. The U-Pb LA-ICPMS data obtained more recently on monazite and the U-Nb-rich mineral indicate a primary mineralisation age (upper intercept) around 462 ±34 Ma (Elburg *et al.*, 2003). The U-Nb-mineral and monazite yield 462 ±14 Ma and 486 ±14 Ma $^{207}Pb/^{206}Pb$ apparent ages respectively.

The No.1 & 2 hematite bodies are intersected by epithermal quartz with minor fluorite veinlets related to the Mt Gee system. Like in several locations around Radium Ridge, magnetite octahedrons pseudomorphosed into hematite have been observed. In all likelihood, the primary mineralisation could have been a hematite-magnetite-monazite lens, later remobilised by a silica-rich fluid of the Mt Gee epithermal system. Oxidised uranium minerals are probably of supergene origin and postdate the epithermal quartz veining. Cadmium is quite elevated in the analysed ore (240 ppm Cd).

SiO_2	TiO_2	Al_2O_3	Fe_2O_3	MnO	MgO	CaO	Na_2O	K_2O	P_2O_5	UO_2	ThO_2	La_2O_3	Ce_2O_3	Nd_2O_3	Y_2O_3	PbO	S	LOI	Sum
18.65	<0.01	<0.01	65.22	<0.01	<0.01	0.05	<0.05	<0.05	4.85	0.50	0.02	3.14	5.41	1.29	0.05	0.02	0.04	0.28	99.58

Table 4: Whole-rock analysis of the hematite-monazite ore at Nr.2 Workings

4.4.2 Migmatitic gneisses from the Radium Creek Metamorphics, Nr.8 Workings crest

The Radium Creek Metamorphics (Coats and Blissett, 1971) near the Radium Ridge and the Mount Gee are composed of metamorphosed sediments (metapelites essentially) with frequent pegmatite intrusions and pegmatitic bodies interpreted to be Paleozoic. The hematitic breccias of the Mount Gee system are associated to this basement Drexel and Major, 1987, 1990).

The samples N8A (0339587/6654573) and N8B (0339687/6655147) were collected on the crest leading to the No.8 Workings. The area is entirely located in the Radium Creek Metamorphics, which are locally formed of quartzo-feldspathic biotite-phlogopite schists, migmatitic gneisses, pegmatitic gneisses and pegmatites.

N8A was collected on flat ground located on weathered biotite-rich gneiss giving a high radioactivity background. The heavy minerals were separated and observed. Ilmenite is the dominant heavy mineral, followed by monazite-(Ce), xenotime, zircon, rutile, apatite and corundum. Apatite, xenotime and monazite are euhedral whereas zircon and rutile are rounded to well-rounded. The zircon typology could only be determined on the less rounded crystals: the "D type" is the most common, a typical feature of the zircons sourced in the local Mesoproterozoic granites.

Because of the strongly dominant proportion of rounded zircons, we interpret they are detrital and this clarify the origin of the gneisses as metasedimentary (paragneisses).

The second sample, N8B, was collected further up along the crest, on a flat ground formed by mica-poor quartz-pink K-feldspar gneiss, with a "granitic look", which lead previous geologists to classify it as an intrusive. The heavy mineral concentrate shows the following mineralogy: magnetite, minor hematite, white zircons (fragmented and rounded) and a very minor proportion of brown euhedral large zircons, minor xenotime and monazite. The rounded zircons morphologies and the quasi-absence of euhedral zircons also indicate a sedimentary origin to this rock. The zircon typologies reveal several D, P5 types of white colour. The sampled outcrop appears as a Pink Pegmatitic "Granite" on the new geological map of Mount Gee (Bons and Rössiger, 2008). The quartzo-feldspathic composition of the rock, its sedimentary HM's assemblage as well as its "granitic" look all indicate the rock composition was probably modified by a K-rich metasomatism.

4.4.3 The "radioactive ilmenite" from the Nr.10 Workings, Mt Gee West

(Broughton, 1925) first mentioned an occurrence of "radio-active ilmenite" in the Mt Painter region at a locality situated between the Main camp in Radium Creek and the No.8 Workings. Coarse crystals of what Broughton calls ilmenite are found shed on the surface of a ridge leading to No.8 Workings. Broughton (1925) also found the mineral in the adjacent biotite schists at the contact of a pegmatite body, as well as within the pegmatite itself, attached to feldspar and quartz. All these occurrences are separated by less than 50-100 meters. The first analyses of the mineral report titanium (56.9 % TiO_2) and iron (22.9 % FeO) dominantly, with uranium and minor vanadium (Broughton, 1925). A fresher sample analysed later give 48 % TiO_2, 5 % U_3O_8 and mention cerium earths (light REE) (Mawson, 1944). As noted by Mawson, the mineral composition is close to the Radium Hill ore: the mineral davidite. The locality is recorded as No.10 by Mawson. However, this number is not kept in the regional mineral inventory where numbering stops at No.9 (Coats and Blissett, 1971). The rather accurate description of the location (½ mile from, and 10° S. of W. of Mount Gee /1½ miles, 5° N. of W. from Mount Painter) was reported on the current topographic maps and the position measured (339675/ 6654725). A geological mapping survey was conducted in 2007 around Mt. Gee and a map produced at 1:2000 scale (Bons and Rössiger, 2008); the position calculated in 2005 was reported on the 2008 map and sits exactly on a folded biotite schist layer in contact with a "Pink pegmatitic granite" body which locally crosscuts the said layer.

The locality was unfortunately not revisited. Instead, some of the samples collected by Broughton were preserved in the South Australian Museum collection (sample G23810) and available for study. The EDS investigations indicate the mineral is davidite-(La). The size of the largest crystals described by Broughton (up to 500 g and 7 cm diameter) also suggests that the davidite mineralisation is of pegmatitic origin. Some of the crystals display large rhombohedra.

LA-ICPMS data were collected on two points devoid of any inclusion on a fresh davidite polished crystal. Average value is 0.46 Wt-% ThO_2 and 5.25 Wt-% UO_2, in accordance with the previous analytical works on the same material in 1944.

4.4.4 Corundum-sapphirine-biotite-phlogopite schists

The corundum-bearing schists have been recognised early on by W.G. Greenwood (1906) in the region of the central Mount Painter; the schist was used to name the "Corundum Creek Schist Member", a sub-unit of the Radium Creek Metamorphics (Coats & Blissett, 1971). The following minerals have been described from the assemblage (Coats and Blissett, 1971, Teale, 1993b): corundum, rutile, phlogopite, biotite, sapphirine, spinel, Mg-chlorite and cordierite whereas the adjacent gneiss hosts sillimanite, gahnite and garnet. The Paleoproterozoic metamorphic peak interpreted by G. Teale (1993) is estimated at 740-760°C and 4.5-5.5 kbar. The Al-rich pelitic rocks provide the best rock composition to record metamorphic event. A sample of corundum schist from the Mount Gee area was selected and crushed for heavy mineral separation; the mineral assemblage recovered is corundum (white, blue, yellow), spinel (red), rutile (dark red), sapphirine (green), phlogopite, and minor zircon (white).

The zircons from this metasedimentary rock display a very unusual morphology: the crystals display a complex growth zoning, with irregular resorption on surface and common black inclusions. Some individuals are melted together, forming irregular aggregates. Some larger zircons still display a "D-type" darker morphology, which clearly differs form the dominant white-pinkish rounded cores of the others. The complexity of the zircons overgrowths probably indicate a HT metamorphic happened; zircon rim formation and crystals aggregation could have formed during either (1) HT anatexis, maybe in granulite facies or (2) could be related to metasomatic remobilisation of Zr. In any of the mentioned scenario, the U-Pb dating of the zircons overgrowths will reveal the age of the HT metamorphic peak/ or metasomatism. The mineral assemblage could also define the pressure conditions (D. Kelsey, oral communication). The Zr-in-rutile and Ti-in-zircon thermometers could also be applied to this assemblage.

4.5 The Paralana Plateau – Hidden Valley Complex regions

The Paralana Plateau and the Hidden Valley Complex form an elongated faulting-thrusting system along the Paralana Fault Zone. Detailed geological mapping and investigation were undergone for the purpose of this research but also as a framework to assess the potential of this area for uranium mineralisations. The integration of this section in the PhD has been approved by Quasar/Heathate.

The studied region extends from the Paralana Hot Springs to the northernmost part of Hidden Valley. The locations of importance are reported on the general geological map of the region (Fig. 23). A complete list of samples can be found in the Appendix III.

4.5.1 The Geology of the Hidden Valley Complex (HCV)

The Hidden Valley Complex (HVC) is described briefly in the geological synthesis on the Mount Painter Province by Coats & Blissett (1971): the valley geology is described as "strongly folded and brecciated sediments in an infaulted outlier", with "dolomitic limestones, coarse-grained massive calc-silicate rocks and thinly bedded, ripple marked quartzites"; all of these are attributed to the Lower Callanna Beds, part of the Adelaide geosyncline sedimentary sequence. "Soda granites and pegmatites" also occur through the valley. The eastern edge of the valley complex is formed by a sub-vertical fault (Lady Buxton Fault) (Coats & Blissett, 1971). The same brecciated Valley Complex is considered as younger by Teale et al. (1993b) and is mapped as Phanerozoic on the included maps. Teale (1993b) reports the presence of vermiculite-talc-chlorite-rich breccia, lower crustal blocks, charnockite, troctolite, anorthosite and calcsilicates. Other breccia complexes also occur to the south of the MPD at a smaller scale (Giants Head intrusion, etc.) and tectonic activity has been interpreted there as Silurian or younger (Lottermoser *et al.* 1988).

The HVC extends from the headwater of the Four Mile Creek (1.5 km wide) to a very narrow band (<10 m wide) disappearing a few hundreds of meters upstream the gorge of the Bottleneck Creek. The HVC reappears further south, to the West of Paralana Hot Springs; the occurrence consists of a narrow elongated breccia body (Fig. 23). The so-defined tectonic unit is mainly composed of Adelaidean metasediments (dolomitic marbles, metadolomites, hornfels, magnetite skarns, tourmaline-bearing chloritized schists, quartzites); regardless to their setting, there are also some mafic volcanics and sediments blocks, mafic intrusives (gabbro, diorites, dolerites or microgabbros), muscovite-bearing granitic pegmatites bodies (largest body: 300 x 150 m), micas-free "soda-rich" leucogranites, blocks of Mesoproterozoic crystalline basement (migmatitic gneisses, micaschists, paragneisses), and blocks of granitic breccia (silicified/chloritized), especially to the south western part of the HVC

The complex can be divided into a series of overthrusts and micro-nappes whose bases are systematically formed by massive breccia. The field recognition of these breccias was investigated in detail by a systematic inspection of the HVC edges and blocks. The breccias from the NW side of the complex are composed of crystalline basement elements and coarsely silicified. So do the "crystalline" tectonic blocks on their thrusting basis. The relative movement of the blocks between each other can be simple or reverse faulted; faults are frequently overlain by massive vuggy quartz veins. The Eastern side of the complex forms an abrupt cliff or steep slope with the metasedimentary breccia being overthrusted by the Mount Neill – Mt Adams granite Unit. The contact here is very sharp, with the presence of granitic (chlorite/hematite alteration) breccias. This feature is systematic all over the 13 km of thrusting contact. The importance of the breccia can easily be underestimated when the breccia is silicified and metasomatised into hard red-coloured "granite-like" rock.

The basement Units on the west of the HVC are the Freeling Heights Quartzite Unit (northern part) and the migmatitic gneisses and schists Unit (southern part). This later unit extends to the SW towards Paralana Hot Springs and even further. The same Unit is named "Radium Creek Metamorphics" in the Southern Mount Painter Inlier. The origin of these gneisses is discussed later. The transition from the Freeling Heights Unit to the Migmatite Unit can be made using radiometrics: the cps readings are 3 to 15 times higher in the latter.

The HVC substratum is interpreted to be composed of both Freeling Heights Unit and Migmatite Unit, as indicated by the tectonic blocks incorporated. The basement "tectonic slices" are themselves intruded by the granite pegmatites and by the gabbros-dolerites. Since these intrusions are present both in the substratum and in the HCV, the whole complex can be interpreted as autochthonous to sub-autochthonous. In some locations, the pegmatite intrusions can be followed regularly in the crystalline basement blocks and abruptly end at the faulted contact with the HVC. This an evidence for a faulting activity after the intrusion of these granitic melts, separating them from their deeper "roots". This records an important Post-Ordovician tectonic activity in the HVC.

The Mafic intrusives

The mafic intrusives occur in the HVC as isolated bodies, frequently associated with blocks of gneisses or as disconnected bodies. The occurrences are observed along eight kilometres strike, both in the basement blocks and in the breccia. Their abundance is remarkable in the context of the MPD, a province dominated by granitoids with minor amphibolites dikes and even rarer coarser gabbroic types. We give here an updated list of the HVC mafic intrusives, including previously reported occurrences in Table 5. This will provide a good starting base for further research on these rocks.

Easting	Northing	Sample	Description
353949	6666083	PW-100	Coarse gabbro, undeformed
354249	6666399	-	Microgabbro
354994	6669029	Gabbro-X	Coarse gabbro (cf. A1015-HV-41 Schaefer)
356672	6670171	GB25	Coarse gabbro (like Gabbro-X), with minor gabbro pegmatite
358119	6672786	JB05-10	Microgabbro – dolerite (Point 1 on Figure 23)
354830	6668070	-	Microgabbro - gabbro/diorite pegmatite
354920	6668180	-	Amphibolite – dolerite
352720	6665740	-	Amphibolite
354136	6666478	PW08-007	Microgabbro (Gb1)
358871	6673202	-	Gabbro chromite-rich (cf. A1015-HV-74, Schaefer)

Table 5: Mafic intrusives in the Hidden Valley Complex region

---

Fig. 23: Geological map of the Paralana Plateau – Hidden Valley Complex regions (next page)

The map was established using the previous geological background, with integration of new structural interpretation and revision through regional mapping at 1:10000 scales. New topographical names have been introduced for the need of this work; the radiometrics have been used on the ground for distinguishing the Th-U-REE-rich migmatitic gneisses and schist. The following sites/samples or groups of samples are indicated: (1) Microgabbro JB05-10, (2) Pegmatitic granite JB06-01, (3) GX01 leucogranite/gabbro pegmatite/gabbro, (4) PEG1 (muscovite-free pegmatite), (5) JB05-21 Calcite-diopside-titanite veins in metasomatized H.V. sediments, (6) Lysandre Cu (Au) mineralisation, (7) Brannerite Hill with Jacob and Charlotte uranium veins, a monazite-hematite pegmatite, (8) A monazite-bearing shear zone, (9) a U/Th=2 metasomatic Mt Neill granitoid, (10) Monazite-zircon-rich biotitites, (11) Soda leucogranite, Hidden Valley-type, (12) syenitic brannerite- and zircon-bearing vein, PW08-001, (12) Monazite Hill mineralisation (biotite schists)

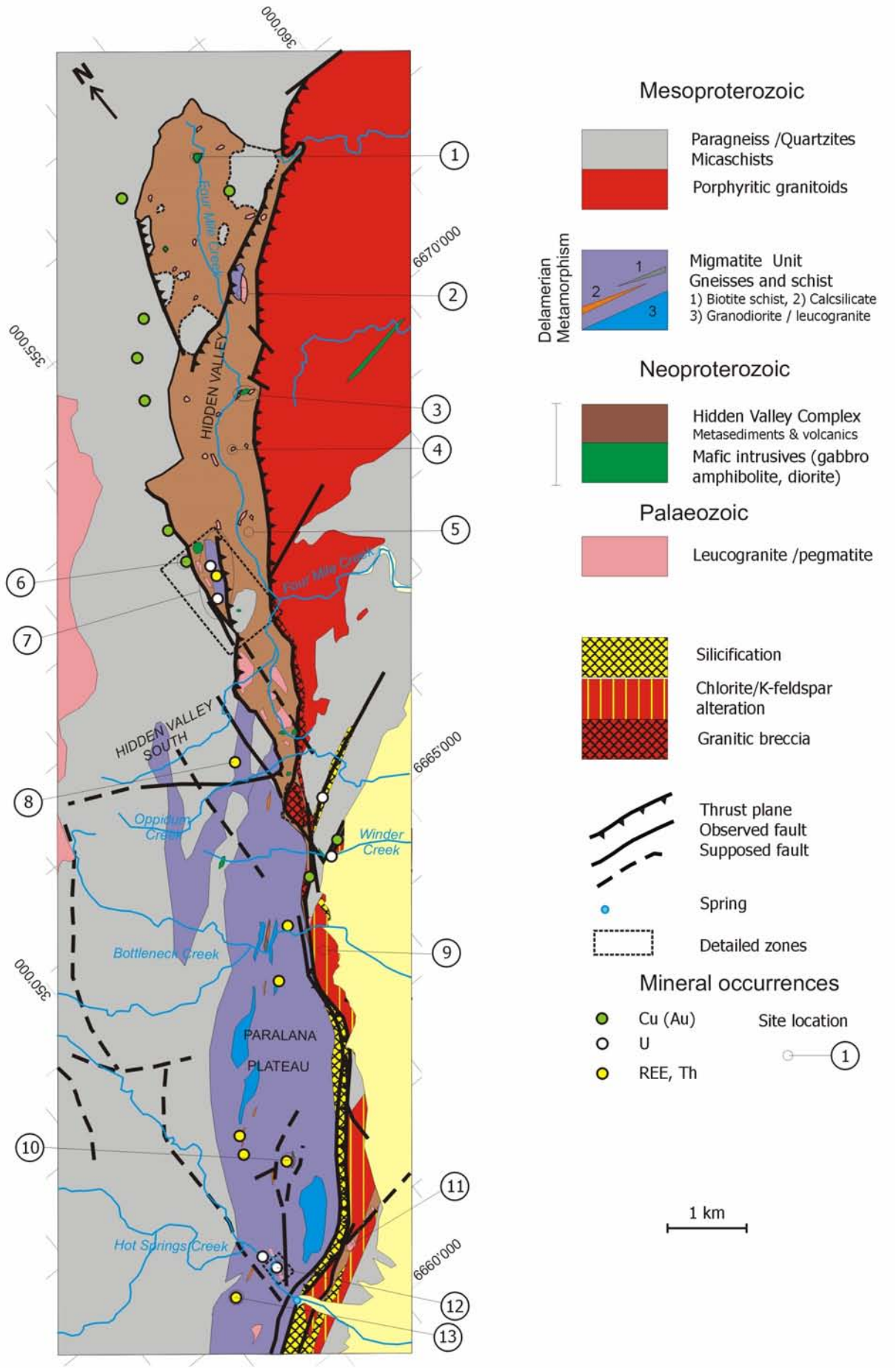
360'000
N
1
6670'000
2
355'000
HIDDEN VALLEY
3
4
5
6
7
HIDDEN VALLEY SOUTH
6665'000
8
Oppidum Creek
Winder Creek
Bottleneck Creek
9
350'000
PARALANA PLATEAU
10
11
Hot Springs Creek
6660'000
12
13
Mesoproterozoic
Paragneiss /Quartzites
Micaschists
Porphyritic granitoids
Delamerian Metamorphism
1
2
3
Migmatite Unit
Gneisses and schist
1) Biotite schist, 2) Calcsilicate
3) Granodiorite / leucogranite
Neoproterozoic
Hidden Valley Complex
Metasediments & volcanics
Mafic intrusives (gabbro amphibolite, diorite)
Palaeozoic
Leucogranite /pegmatite
Silicification
Chlorite/K-feldspar alteration
Granitic breccia
Thrust plane
Observed fault
Supposed fault
Spring
Detailed zones
Mineral occurrences
Cu (Au)
U
REE, Th
Site location
1
1 km

The mineralogy of the microgabbro JB05-10 was studied in detail and gives the following percentages: labradorite 50%, augite 35%, hypersthene 15% and magnetite 1%; the fabric is granular with even distribution of minerals. Geochemically, the rock presents similar patterns than the amphibolite dikes form the MBI with slightly higher HFSE concentrations (169 ppm Zr, 14 ppm Nb and 48 ppm Y).

Anorthosite or plagioclasite

To the west of Brannerite Hill, a large outcrop of pure oligoclase-andesine rock (anorthosite) was discovered, adjacent to a gabbro body. This gabbro-anorthosite layered intrusion forms a lenticular shaped body. The gabbro is formed of hornblende, hypersthene, and plagioclase essentially and the anorthosite appears devoid of ferromagnesian. Although the rock looks leucocratic, it strongly differs from the quartz-bearing "soda-rich" leucogranites occurring in the HVC. The rock also contains two accessories: ilmenite and rutile. Unidentified small red crystals are observed in it and could be spinel, ruby or baddeleyite; this requires verification. The plagioclase composition determined by EDS is An22 - Ab69.5 - Or8.5; this K-rich plagioclase composition is indicating a high temperature of crystallisation (> 700-800°C), in accordance to its mafic igneous origin (Hébert, 1998). The whole-rock XRF composition slightly differs from the EDS analyses and indicates an average of An29.2 – Ab60.4 – Or10.3 (andesine); most trace elements are <10 ppm except Sr (140 ppm).

The "soda-rich" leucogranites

The HVC hosts numerous small intrusive bodies of "soda-rich" leucogranites; these bodies are generally formed of very coarse, pegmatitic K-feldspar, quartz and oligoclase. These rocks are distinctive from the typical mica-bearing coarse pegmatites related to the British Empire Granite (BEG). They also appear to the South of the MPI, intruding the basement around the Sunshine Pound and the Bob's Knob (G. Teale, oral communication 2008) as well as intruding the Adelaidean sequence at the Sitting Bull, The Needles, The Pinnacles, Giant's Head and Tourmaline Hill. These intrusions were interpreted as "high-level cupola-like projections from an extensive subsurface igneous mass" (Mawson and Dallwitz, 1945).

Rb-Sr dating using K-feldspar and muscovite have been realized on these rocks (unpublished data, Teale 1979; Elburg et al. 2003). A supposed U-Pb age at 372 ±2 Ma is erroneously reported by Preiss (1995) and mentioned again with an additional transcription error in Elburg et al. (2003). The original data was kindly communicated by G. Teale: it consists of muscovite - whole-rock Rb-Sr isochrone ages are 450 ± 4 Ma ($^{87}Sr/^{86}Sr$ 0.7125±0.0010) at the Sitting Bull & Pinnacles; 418 ± 2 Ma (0.7441±0.0004) at the Giant's Head and 372 ± 2 Ma (0.7251±0.0004) at the Needles. Unlike mentioned by Preiss (1995) and Elburg (2003), U-Pb dating was never applied to these rocks. The brecciation of the HVC dissected some of the "soda-rich" leucogranites and therefore indicates they predate this tectonic phase.

During the course of the Hidden Valley mapping, more than fifty individual bodies of "soda-rich" leucogranites or pegmatites were recorded.

A graphic pegmatite was studied in detail in the central part of the Hidden Valley (PW-160A-D, locality 4 on Fig. 23). The body intrudes a locally preserved sedimentary block of HCV sediments (marble, metadolomites and quartzites). The granite pegmatite consists of coarse graphic quartz-plagioclase. K-feldspar is absent. The plagioclase is sodic (albite-oligoclase) and untwinned. Veinlets of fluorite (<1 mm) crosscut the rock. Apatite was also observed. Zircon is absent. The dolomitic marble close to the intrusion (<1 m) is an impure siliceous carbonate sediment. The following minerals are present: dolomite, quartz, riebeckite and very little tremolite. The marble is in turn transitionally getting into a coarse magnetite skarn, with large (~1 cm) euhedral magnetite crystals. Late fracturation occurs at both microscopic and outcrop scales. The sodic amphibole (riebeckite) is displaying an acicular-fibrous texture and probably results from a Na-metasomatism related to the granitic intrusion.

A new occurrence of "soda-rich" leucogranite was found out of the HVC, east of Paralana Hot Spring, in the metasomatized fault zone near Paralana Fault Hot Springs (Fig. 23), (PW08-032 and PW08-033). The outcrop consists of a large body of granite/pegmatite formed of albite, quartz and K-feldspar. The localization of the body was made during the inspection of an airborne U>Th anomaly confirmed on ground using a gamma spectrometer. The intrusions are associated with carbonate-rich and phlogopite-bearing breccia, similar to the lithologies in the HVC to the north. The outcrop is interpreted as the southernmost extension of the HVC. Like elsewhere in the MPD, quartz-feldspar graphic texture can be observed in the more pegmatitic zones. The leucogranite is auto-brecciated and rounded clasts of coarse granite are embedded in albite-rich finer matrix. It indicates the body intruded during a period of active faulting. Fluorapatite is a common accessory mineral, occurring as < 1 mm anhedral green grains. This later mineral was only observed in the albite-rich zones.

Muscovite-bearing pegmatites and granites

The second category of granite pegmatites is relatively richer in microcline and quartz than the "soda-rich" type. The presence of muscovite was frequently recorded but also spessartine garnet is some location. Many of these bodies have been mapped and only limited locations were investigated in detail. One of them was selected for geochronology purpose: a large pegmatite body intruding into a migmatitic basement block in the Hidden Valley

North (JB06-01, LI-PEG, location no. 2 on Fig. 23). The rock consists of a coarse granite pegmatite with pink K-feldspar, oligoclase, quartz and abundant muscovite. The texture is graphic but tends to a normal granitic grained rock in some areas. The composition frequently grades to muscovite-rich concentrations showing an arborescent texture, as frequently met in the pegmatites crosscutting the BEG. The accessory minerals separated from a crushed sample are: xenotime-(Y), rutile, ilmenite and rare rounded inherited zircon. The xenotime was used to date the intrusion.

Another major pegmatite dike outcrops on the eastern side of a paragneiss-micaschists block, SW from Brannerite Hill. The dike can be followed along 400 m. The vein appears discontinuous and the segments are generally shifted by several tens of meters vertically or transversally. This records the post-intrusion faulting and thrusting movement in the HVC (Fig. 24). Another example from the South of the HVC is observed along the brecciated mix under the overthrust of the granitic breccia (Fig. 25). Several blocks of micaschists basement are scattered in the complex. Two of them have muscovite pegmatites intruding them. However these pegmatite and their hosting blocks are totally un-rooted from their substratum. In the same area, all floating individual pegmatites bodies from the HVC are mica-free and rich in albite.

Hornfels and contact metasomatism

Many outcrops of the HVC are metamorphosed in the hornblende hornfels or the amphibolite facies; mineral assemblages from the carbonates-rich sediments display calcite, dolomite, tremolite, diopside, very minor grossularite, and phlogopite, Na-K rich scapolites in the more metasomatised sediments. Overall the HVC display all the characteristics of the amphibolite facies ($T > 500°C$ /$P > 2$ kbar). The intensity of the fluid alteration and metasomatism is however highly variable, also due to the heterogeneity of the breccia complex.

A locality in the central HVC was studied more in detail (JB05-21, locality 5 on Fig. 23); a rocky hill composed of dolomitic sediments forms the hill, crosscut by a pegmatite body (soda-rich leucogranite) over 10-25 m in diameter. Several veins of calcite-diopside-scapolite crosscut the sediment, less than 10 m away from the pegmatite. The metamorphosed sediments mainly consist of Na-K scapolite (near marialite end-member), diopside, calcite and dolomite. Other minor phases are grossularite garnet, which occurs as anhedral crystals (<100 μm), titanite, occurring as disseminated small euhedral crystals (up to 1 mm in the calcite vein footwalls), apatite prisms (up to 3 mm) and andesine (mainly associated with the scapolite). The age of the metamorphism will be discussed in the geochronology section, with U-Pb data obtained on the titanite from the calcite veins.

Heavy minerals separated from several gullies in the brecciated sediments can be separated in several groups: (a) phlogopite-tourmaline, (b) pyrite-tourmaline, (c) magnetite and (d) rutile. Apatite and rounded white zircons are widespread in the sediments. Rutile from some of the sediments is coarse, euhedral with smoothed corroded edges. This feature could be related to the metasomatic fluids.

4.5.2 Geology of the migmatitic gneisses and schists Unit

The main rock unit forming the Paralana Plateau and its north-eastern extension to the HVC is composed of metamorphosed quartzo-feldspathic gneisses, biotite gneiss, biotite schists (biotitites), minor calc-silicates layers, cordierite-bearing quartzites and phlogopite schists (Blight, 1977, Teale, 1993b). The rocks frequently display an alternation of leucomes and restitic schists at a meter scale, a common characteristic of migmatites. The lithologies have been described in detail by the pre-mentioned authors and are generally consistent with the field observations made during the field works. The most common gneisses from the migmatitic unit contain biotite, magnetite and sillimanite. Many of the leucogranites (leucosome) from the migmatitic unit are rich in sodic plagioclase, which contrasts with the composition of the restitic material that is devoid of feldspars and composed of more than 80% biotite. Locally, pink layered biotite gneisses (rich in K-feldspar) display more granitic compositions. This migmatitic Unit is in all respects similar to the gneisses and schists from the Radium Ridge-Mount Gee area; they may mainly differ by a higher intensity of the pegmatites intrusions.

Calcsilicates

The more calcic rocks of the unit are: (a) granodioritic gneisses and (b) calcsilicate layers. Both contain allanite-(Ce), which can form some local concentrations. Some of them, especially in the Bottleneck creek bed, reach several percents and have been reported as REE indices on the map (Fig. 23). The calcsilicates are formed of diopside, andesine plagioclase, allanite-(Ce), hastingsite, magnetite, garnet and titanite. These horizons are generally discontinuous but of regular appearance along some strikes; they are interpreted as metasomatised carbonates layers.

Biotitites and biotite schists

The biotite schists from the Paralana Plateau are generally rich in heavy minerals: zircons, monazite, xenotime, sillimanite and magnetite. Their higher density is due in part to the high content of heavy minerals but mainly to the dense biotite rock-forming mineral. These layers are interpreted as extreme restitic material. Concentrates of heavy minerals from pure biotitites show high REE, Th and P contents related to ~3 Wt-% Th-rich monazite and 0.5 Wt-% zircon.

4.5.3 Complimentary data from the Bottleneck Creek sediments

Additionally to the mapping works realized on the outcrops, a large sample of sediments draining the watershed of the Bottleneck Creek was used to quantify the global distribution of the heavy minerals (a), with a special interest for the radioactive minerals and also the statistical age distribution of zircons and monazites. A careful inspection of the radioactive cobbles was undergone on a 100 x 50 m surface with a scintillometer, in order to locate disseminated mineralisations; (b) a mineralised cobble was studied mineralogically and petrographically

(a) FMC heavy minerals:

The heavy mineral population from the sample FMC, already described as a comparative sample for zircon typology during the study of the Beverley uranium deposit sands, are issued from the restricted watershed of the Bottleneck Creek. The source rocks are the migmatitic gneisses unit (55%), the Freeling Height Quartzite (40 %) and the "I-type" tail of the British Empire granite. Due to the relative poverty in heavy minerals from the last two units, it is assumed the HM's assemblage principally comes from the Migmatitic gneisses and schists. The Following minerals were recovered out of 322 g of HM's: ilmenite & hematite (60 %), magnetite (31 %), monazite, xenotime (3 %), allanite (~1 %), garnets (0.5 %), zircon (2 %), rutile, brookite (0.8 %), apatite (0.6 %), sillimanite (0.2 %), minor fluorite, clinozoizite-epidote, corundum, scheelite, tremolite, hornblende. Kyanite was not observed.

(b) FMC-cobble:

The rock is an alkali-granite, formed of quartz, microcline, minor oligoclase and scattered subparallel biotite. Accessories are allanite, xenotime, zircon, magnetite and polycrase-(Y). U-Pb dating of these polycrase and zircon are reported further.

4.5.4 Geology of the Brannerite Hill

An elongated tectonic block from the central HVC named "Brannerite Hill" is composed of migmatitic gneisses, schists and pink K-rich highly metasomatised gneisses. This block of basement has the same major lithologies and similar radiometric signatures with elevated Th and U than the Migmatitic Unit from the Paralana Plateau. Several uranium and REE mineralisations were found in it (Fig. 24). The block has the shape of a finger measuring 900 by 180 m. The lithologies tilt toward the SW, due to the anti-clockwise rotation of the block on 90-110° relative to the migmatitic unit further south. The surrounding HVC sediments record the movement with shearing and folding, especially to the north-east corner of Brannerite Hill where a block of stratified sediments is in direct contact with it.

A series of migmatitic biotite red gneisses layers with high Th-U content (200-300 ppm Th) alternate with the quartzo-feldspathic biotite gneisses. A succession of biotitites and leucogranitic layers is frequently observed at a metric scale. At the scale of the migmatitic unit, these leucosomes/melanosomes have probably not migrated very far away. The thickness of these layers varies from 5 to 80 m. Several N-S faults subdivide the hill in four segments, which are considered to be shifted vertically between each other. The lowest compartment is probably the western one, which displays the strongest metasomatic alteration and recrystallisation into a microcline-quartz-hematite assemblage. Muscovite-rich pegmatites or leucogranites dikes (related to BEG) crosscut the gneisses getting more abundant toward the eastern compartment. They clearly predate the main faulting and segmentation of the block. The same observation can be made for the hill to the South of Brannerite Hill where a major pegmatite dike is segmented along 400 m.

Associated with the N-S faults and the thrusting planes (140°N/30-50°) are massive to vuggy quartz veins with K-feldspars (replacing a earlier fibrous mineral). The contacts are locally brecciated. Several mineralisations in brannerite or monazite have been discovered in it. Elsewhere in the Freeling Height Unit basement, similar veins have been observed, with ilmenite layering and pegmatitic amphiboles (up to 1 meter crystals) pseudomorphosed into K-feldspar.

4.5.5 Uranium, thorium and REE mineralisations

Numerous high-REE, -U, -Th disseminations are widespread in the migmatitic gneiss unit. Additionally, several mineralisations with U, Th or REE expressed in percents were discovered. The Brannerite Hill is named after the discovery of three distinct uranium mineralisations spread along a 500 m strike on the side of a hill crest. Two monazite mineralisations were also discovered: one in the core of the Brannerite Hill and a second in a shear zone in the migmatitic gneisses unit. Finally, a third type of mineralisation is described here: an alkaline syenite vein (20 cm wide) mineralised in brannerite.

Alkaline syenite brannerite-bearing vein

The mineralisation is of small size and with restricted extension. However, because of its unique type in the province, special attention is given to it. The mineralised vein occurs in the middle of Hot Springs Creek bedrock (Fig. 27); it crosscuts the hosting migmatitic gneisses, driven aside from a large tourmaline-, muscovite-bearing pegmatite dike (10-20 m wide). The temporal link between the pegmatite and the vein is still uncertain. The vein is coarse to

medium-grained and contains mainly albite (60%), K-feldspar (35%), quartz (1-2%), biotite (3%) and calcite, corresponding to alkaline syenite in the QAPF Streckeisen classification. Accessories are skeletal magnetite, brannerite, gummite, euhedral zoned zircon and an alkaline amphibole displaying agpaïtic texture. The gamma spectrometry indicates a U/Th of 4. Brannerite crystals form egg-shaped or circular crystals from 0.5 up to 30 mm. The vein reaches 1500 cps whereas the surrounding migmatites give a background of 300-400 cps (biotite-rich types) down to 250-150 cps in the leucocratic types (plagioclase-rich). The pegmatite dike shows the lowest counting (100 cps).

A sample of the radioactive brannerite was examined by EDS and found to be nearly pure UTi_2O_6. The XRD indicates that the mineral is metamict. Another sample was heated at 800°C for 6 h under inert atmosphere and again prepared for XRD; the results confirmed brannerite but indicate it is mixed with an unknown phase, possibly microlite. Additional brannerite was also found a few hundred of meters upstream in smoky quartz fault planes and mentioned by Coats & Blissett (1971).

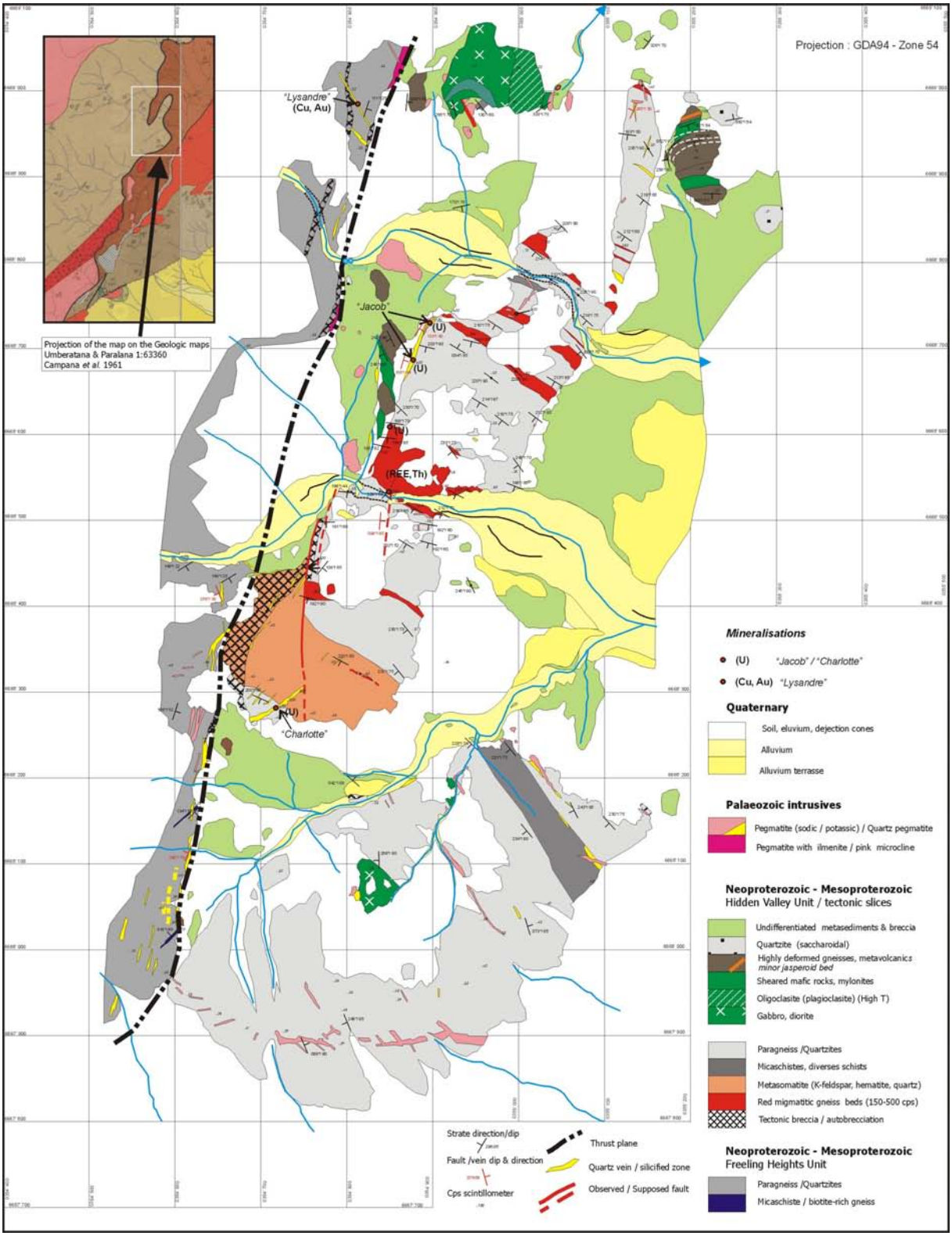

Fig. 24: Geological map of the Brannerite Hill area

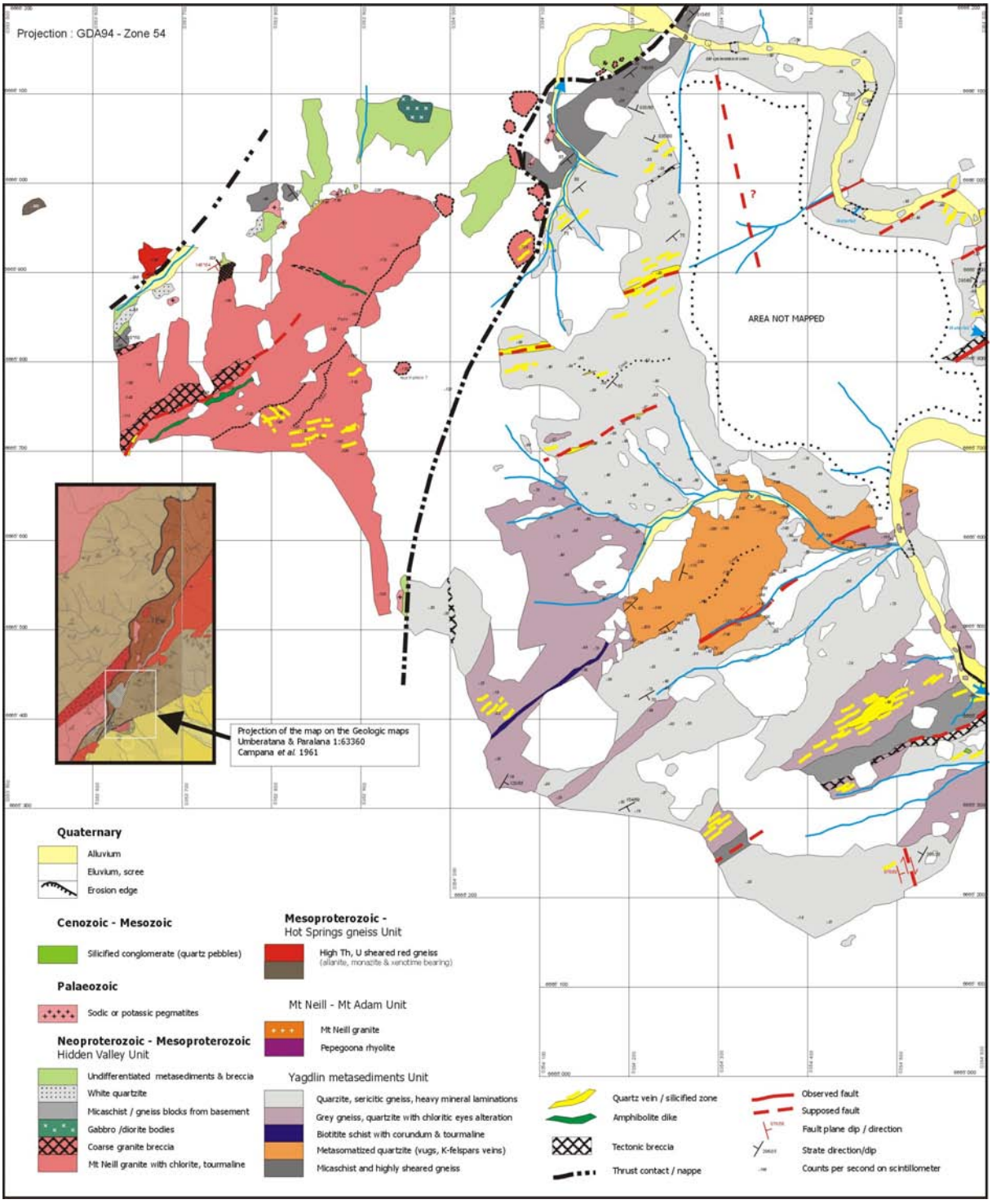

Fig. 25: Geological map of the Southern HVC and the Oppidum Creek gorge

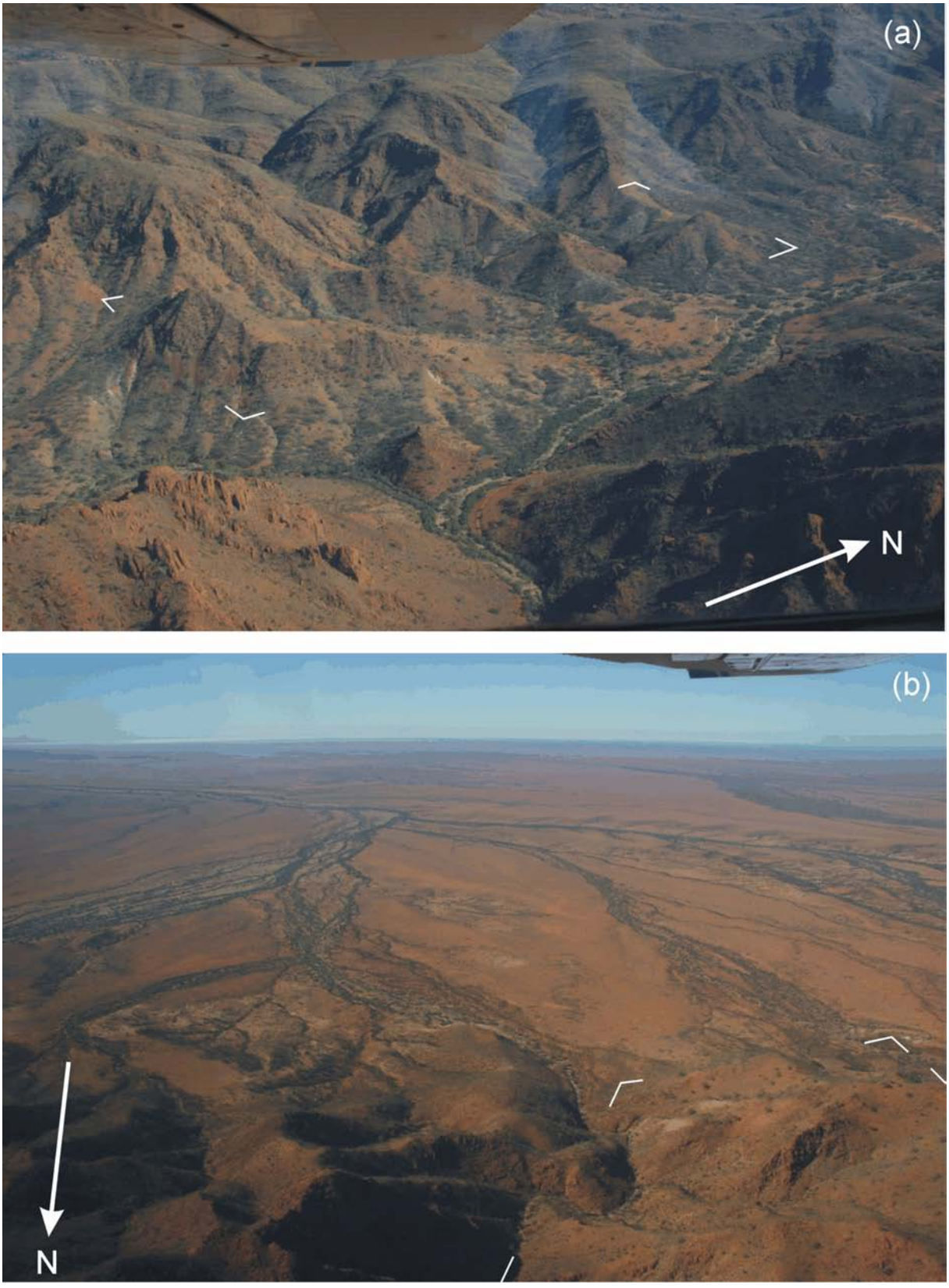

Fig. 26: Pictures of the Brannerite Hill and the Oppidum Creek gorge

The maps from figures 24 and 25 are projected on these two aerial pictures kindly provided by David Haberlah; (a) View of the HVC with the Four Mile Creek entering the Mount Neill-Mount Adams Unit (in front); Brannerite Hill and the southern hill in the selected area; the Freeling Height Unit and the edge of the British Empire granite at the back; (b) Oppidum Crrek (at the front) joining the Four Mile Creek in the plain; the steep outcrop in the centre of the selected area is highly silicified quartzite and micaschists.

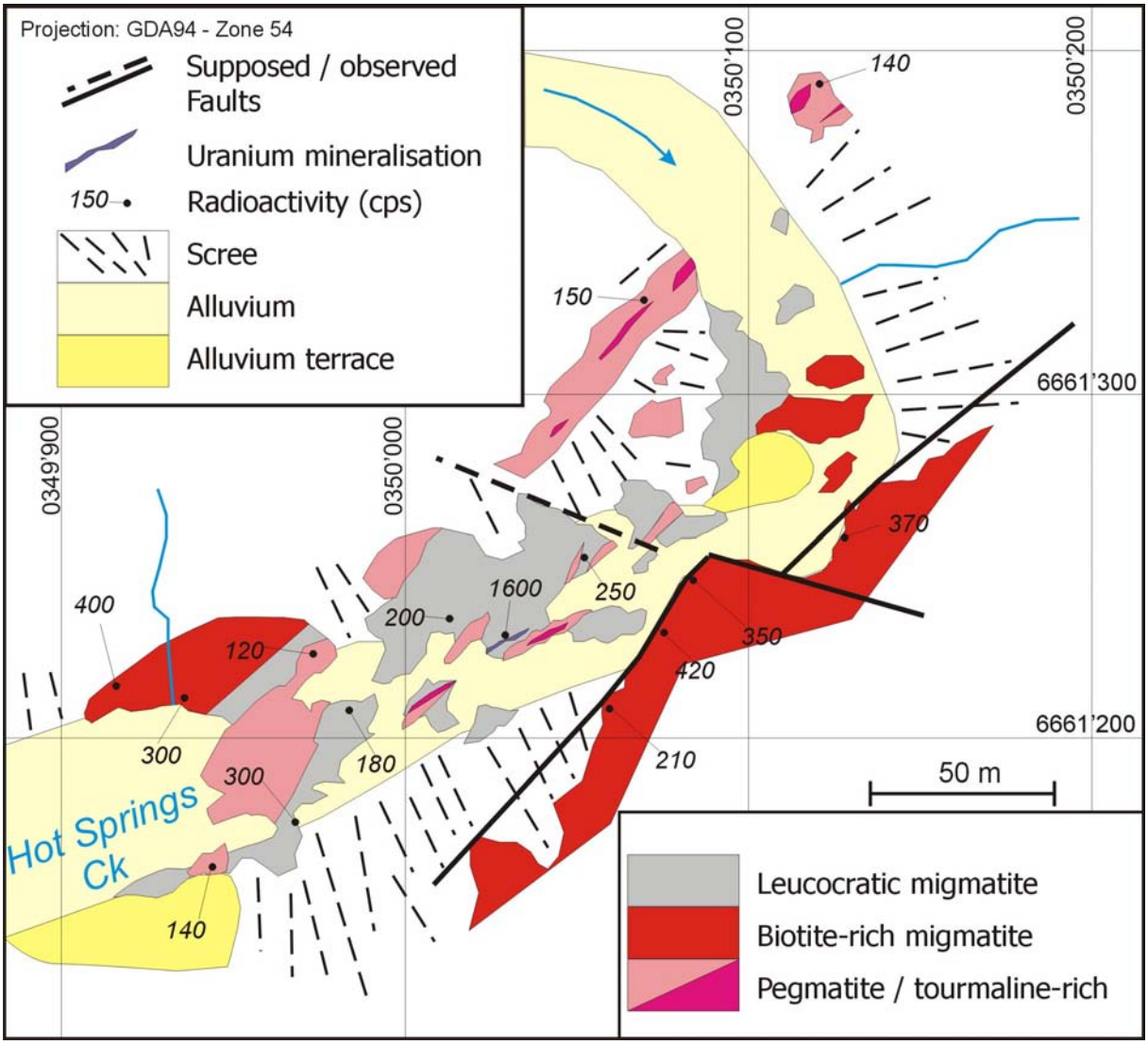

Fig. 27: Geological map of the Hot Springs Creek gorge brannerite mineralisation

Quartz-brannerite-ilmenite veins (Charlotte, Jacob)

The mineralisations of Brannerite Hill were discovered when examining some smoky quartz samples found on the Western side of hill. Since the original find, several quartz veins of similar nature have been discovered in the area. Many of them only host ilmenite (Fig. 24), and brannerite mineralisation was recognised at only three localities. The mineralisations form two distinct groups, separated by around 400 m; the southern mineralisation is called "Charlotte" and the northern one "Jacob". The ilmenite-bearing veins are located at the contact of the HVC, in the Freeling Height Quartzite Unit.

The main mineralisation "Jacob" is located on the western flank of the Brannerite Hill, in the quartz vein sealing the fault at the contact with the HVC (Fig. 28b). The vein is either formed of massive vuggy quartz or of pegmatitic K-feldspar, quartz, ilmenite with lesser amounts of muscovite and Mg-rich amphibole (now transformed into clinochlore + sericite). Amphibole forms locally pegmatitic spreading up to 20-30 cm in length. The development of amphibole is mostly located at the vein contact with the Mg-rich HVC sediments. The vuggy nature of the quartz-rich intervals indicates that the vein emplaced at shallow depth. Many of the quartz crystals were broken and healed during growth. Brannerite concentrations are extremely variable, locally reaching more than 20 vol-% in brannerite. The quartz in the vicinity of brannerite is smoky, due to the radiation damage. At Charlotte, brannerite occurs as small isolated needles disseminated in the quartz matrix (<1 vol-%). Brannerite at Jacob forms long striated prisms up to 12 cm in length (Fig. 28d & h).

The mineralisation at Charlotte contains more ilmenite-(hematite) than brannerite and is poor in K-feldspar. This provides an excellent link between Jacob and the barren ilmenite pegmatites. The ilmenite-bearing veins are clearly "pegmatitic". The size of the crystals reaches exceptional dimensions: ilmenite forms layers of 2-5 cm thick along several meters (Fig. 28g), with large, perfectly formed dodecahedra. The pink K-feldspars reach 40 cm and amphiboles (now transformed in feldspars) up to 1 meter. The striation of the early amphibole is always overprinted on the ilmenite crystals, and crystal relationship indicates "amphiboles" crystallised early in the sequence. The vein history includes several stages of faulting and fluid/melt introduction in the same dynamic context than the brannerite mineralisations.

Monazite veins and shear zones

Monazite concentrations are not uncommon in the Migmatite Unit and occur generally in close association with biotite-rich schists or gneisses. Monazite mineralisations with percent grades are mentioned on the online database of the South Australian Mine Department (PIRSA) around Paralana Hot Springs in biotite schists (Monazite Hill). We found similar mineralisations with high Th counts on the scintillometer were found in a shear zone, in the Hidden Valley South area (PW08-008) and on the top of the Paralana Plateau (PW08-027). The origin of these REE concentrations seems to be directly linked to the migmatite genesis and the concentration of monazite in the restitic material.

A different type of mineralisation was found in the middle of the Brannerite Hill basement block, along a fault zone (PW-211). The mineralisation is hosted in a breccia formed of gneiss and muscovite-bearing pegmatite elements. The mineralisation includes large monazite crystals and masses (Fig. 29d), hematite, quartz, Co-rich pyrite, chlorite and thorite. The paragenesis and the style of mineralisation (in a brecciated zone) indicate analogies with the U-REE Radium Ridge No.2 and the Mt Gee deposits. The presence of muscovite pegmatite (BEG related) in this breccia provides a maximum age.

Allanite concentrations

Allanite-(Ce) is a widespread mineral in the Migmatitic Unit. It was recognised in the biotite-magnetite gneisses and in calcsilicates rocks. The size of allanite generally varies from hundreds of μm to 5 mm, exceptionally reaching 2-3 cm. The presence of calcsilicates mineralised in REE-(Th-U) similarly to the formations met in the Brindana Gorge region suggests that the metasedimentary rocks were metasomatised. In three locations from the Central Paralana Plateau, allanite was found in calcsilicates, together with magnetite (All-2, PW08-002, BRA12) (Fig. 29). More rarely, allanite crystals display large epidote rims (Fig. 29b).

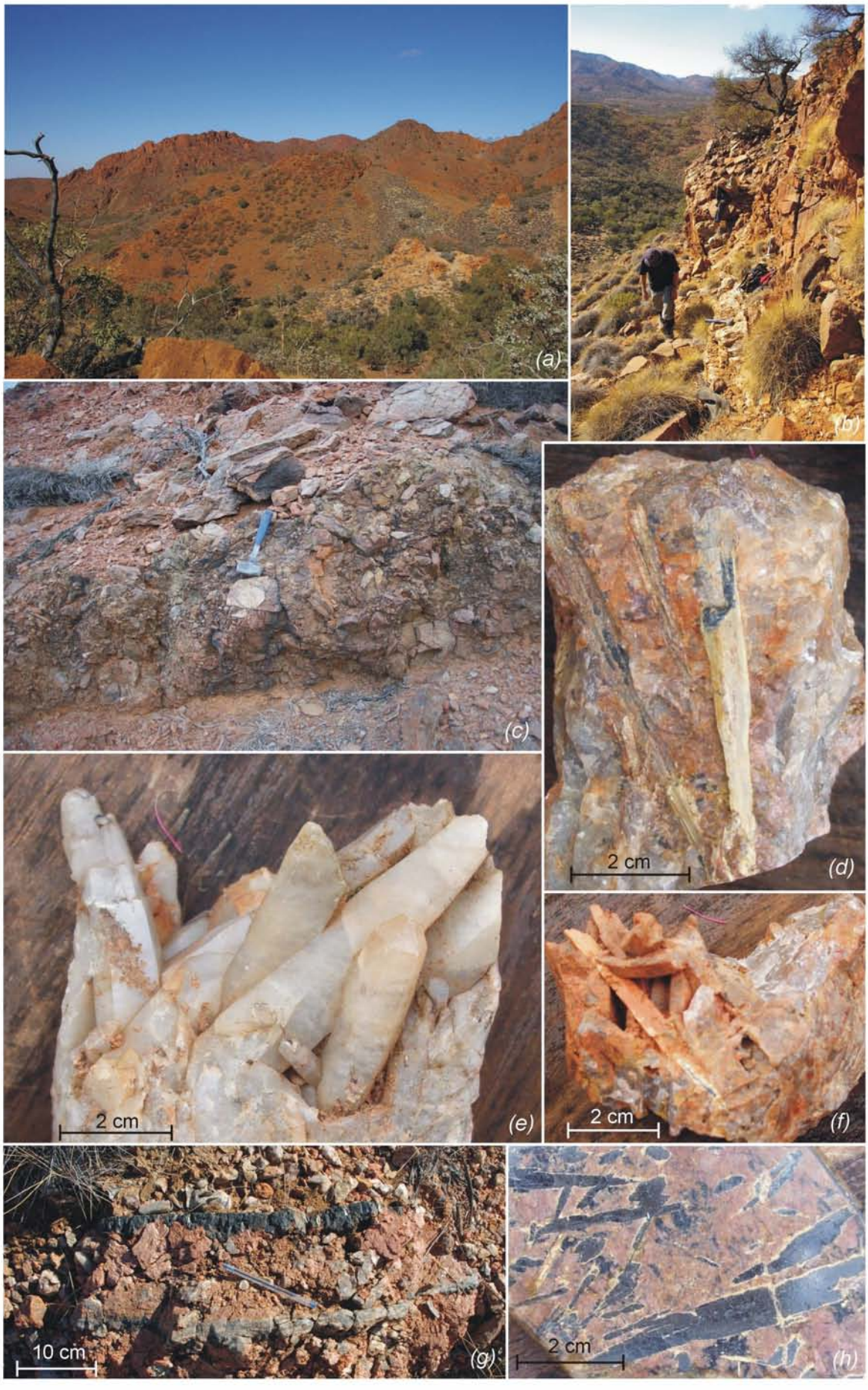
(a)
(b)
(c)
(d)
2 cm
(e)
2 cm
(f)
2 cm
10 cm
(g)
2 cm
(h)

Fig. 28: Mineralisations from the Brannerite Hill – Hidden Valley Complex *(previous page)*

(a) View of the small valley behind Brannerite Hill with the leucogranite-pegmatite intrusion (in white); the rocky spur several tens of meters below the hill top underlines the "Jacob" fault/vein mineralisation. The mountains at the back belong to the Mt Neill-Mt Adams Unit. The Hidden Valley outlet is visible on the left; (b) Sub-vertical quartz vein at "Jacob" (looking to the northeast); the slope on the left is formed of brecciated Mg-rich metasediments from the HVC; (c) Massive tectonic breccia composed of crystalline basement boulders and cobbles (Hidden Valley northwest overthrusting contact); (d) brannerite needles in a quartz-microcline matrix (pseudomorphosed from amphibole); note the marked striation; (e) Large smoky quartz crystals from the "Charlotte" mineralisation; the crystal on the left was fractured and resealed during its growing stage;(f) brannerite needle in an open vug (yellow alteration);(g) large ilmenite layering from a pegmatite vein at the faulted contact between the Freeling Heights Quartzite Unit and the HVC, west of Brannerite Hill; (h) polished slab of mineralisation at "Jacob" with large brannerite crystals in a microcline matrix.

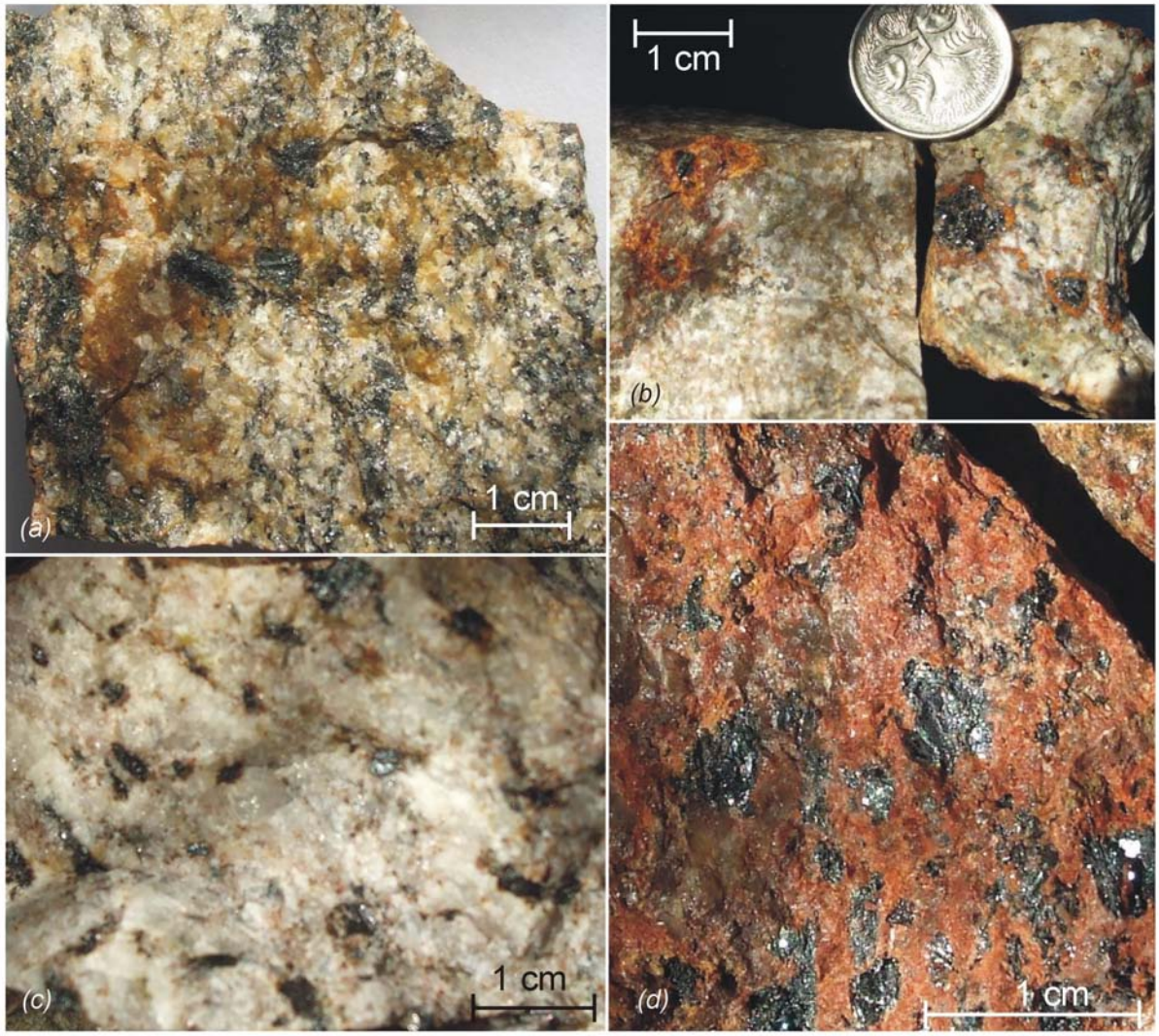

Fig. 29: Pictures of REE mineralisations from the Brannerite Hill – Hidden Valley Complex

(a) Magnetite biotite allanite-(Ce) granodioritic gneiss from the Bottleneck Creek gorge (PW08-029); (b) large centimetre-size allanite crystals rimmed by epidote-zoisite in a coarse-grained metasomatised sediment on the western side of Paralana Plateau; (c) Allanite from a quartzo-feldspathic gneiss with magnetite (All-2); the sample was collected in the central part of the Paralana Plateau, in the Bottleneck Creek watershed; (d) coarse monazite (40%) (red-orange) mixed with hematite, quartz and muscovite (PW-211); the original pegmatitic structure is partly preserved.